ISTANBUL TECHNICAL UNIVERSITY ★ GRADUATE SCHOOL OF SCIENCE ENGINEERING AND TECHNOLOGY

VISIBLE LIGHT-INDUCED COPPER(I)-CATALYZED AZIDE ALKYNE CYCLOADDITION WITH ZINC OXIDE SEMICONDUCTOR NANOPARTICLES

M.Sc. THESIS

Kadriye Özde YETİŞKİN

Department of Chemistry

Chemistry Programme

DECEMBER 2015

ISTANBUL TECHNICAL UNIVERSITY ★ GRADUATE SCHOOL OF SCIENCE ENGINEERING AND TECHNOLOGY

VISIBLE LIGHT-INDUCED COPPER(I)-CATALYZED AZIDE ALKYNE CYCLOADDITION WITH ZINC OXIDE SEMICONDUCTOR NANOPARTICLES

M.Sc. THESIS

Kadriye Özde YETİŞKİN
(509131023)

Department of Chemistry

Chemistry Programme

Thesis Advisor: Prof. Dr. Yusuf YAĞCI
Anabilim Dalı : Herhangi Mühendislik, Bilim
Programı : Herhangi Program

DECEMBER 2015

İSTANBUL TEKNİK ÜNİVERSİTESİ ★ FEN BİLİMLERİ ENSTİTÜSÜ

ZnO YARI-İLETKEN NANOPARTİKÜLLERİ KULLANILARAK HETEROJEN FOTOKATALİZ SİSTEMİ İLE AZİD-ALKİN ÇIT-ÇIT REAKSİYONU

YÜKSEK LİSANS TEZİ

Kadriye Özde YETİŞKİN
(509131023)

Kimya Anabilim Dalı

Kimya Programı

Tez Danışmanı: Prof. Dr. Yusuf YAĞCI
Anabilim Dalı : Herhangi Mühendislik, Bilim
Programı : Herhangi Program

ARALIK 2015

Kadriye Özde Yetişkin, a **M.Sc.** student of ITU **Graduate School of Science Engineering and Technology** student ID 509131023, successfully defended the **thesis** entitled "**VISIBLE LIGHT-INDUCED COPPER(I)-CATALYZED AZIDE ALKYNE CYCLOADDITION WITH ZINC OXIDE SEMICONDUCTOR NANOPARTICLES**", which she prepared after fulfilling the requirements specified in the associated legislations, before the jury whose signatures

Thesis Advisor :	**Prof. Dr. Yusuf YAĞCI** Istanbul Technical University	.....
Jury Members :	**Prof. Dr. Gürkan HIZAL** Istanbul Technical University	.....
	Prof. Dr. M. Atilla TAŞDELEN Yalova University	.....

Date of Submission : 27 November 2015
Date of Defense : 23 December 2015

To my family,

FOREWORD

First and foremost, I would like to thank my supervisor Professor Yusuf Yağcı for his guidance, great support and kind advice throughout my MSc research studies. It was a real privilege and an honour for me to be working under the supervision of him and to share of his exceptional scientific knowledge. Thanks for giving me a lot of inspiration on how to become a better scientist.

My sincere gratitude goes to Sajjad Dadashi-Silab for helping me solve so many problems and providing me with many insightful suggestions. Without his involvement, this work would not have been possible. Everytime, he guided me in many issue and helped me with his kind patience.

I also need to thank past and current members of Yağcı Research Group. I wish to deeply thank to Dr. Hüseyin Akbulut who never hesitated to put forward his valuable support; and a special thank to Merve Kara for her friendship from very beginning. I also wish to thank Assoc. Prof. Mehmet Atillla Taşdelen, Dr. Demet Göen Çolak, Dr. Ioan Cianga, Dr. Ömer Suat Taşkın, Dr. Sean Doran, Res. Asst. Mustafa Arslan, Res., Res. Asst. Ali Görkem Yılmaz, Asst. Mustafa Çiftçi, Res. Asst. Yonca Alkan, Cansu Aydoğan, Eljesa Murtezi, Eliften Semerci, Senem Körk, Semih Erdur, Ceren Kütahya and Recep Erdem Ahan with all of you, it has really been a great pleasure.

Finally, I reserve special thanks to my family for their encouragement, understanding, patience, love and all the support they have provided me over the years. They have been my motivation for continuing to improve my knowledge and move my career forward.

Thank you all very much.

TABLE OF CONTENTS

Page

FOREWORD ..... **ix**
TABLE OF CONTENTS ..... **xi**
ABBREVIATIONS ..... **xiii**
LIST OF TABLES ..... **xv**
LIST OF FIGURES ..... **xvii**
SUMMARY ..... **xix**
ÖZET ..... **xxi**
1. INTRODUCTION **1**
2. THEROTICAL PART **3**
2.1 Click Chemistry 3
2.1.1 Copper(I)-catalyzed azide-alkyne cycloaddition reactions (CuAAC) 4
2.1.1.1 The catalytic system 6
2.1.1.2 Mechanism 14
2.2 Nanomaterials And Zinc Oxide Nanoparticles 16
2.2.1 Properties of nanomaterials 16
2.2.2 Zinc oxide nanoparticles (ZnO NPs) 17
2.2.3 Crystal structure of zinc oxide 18
2.2.4 Synthesis of ZnO nanoparticles 19
2.2.5 Applications of zinc oxide 23
3. EXPERIMENTAL PART **25**
3.1 Materials 25
3.2 Instrumentation 25
3.3 Preparation of Zinc Oxide Nanoparticles (ZnO NPs) 27
3.4 Procedures for the Preparation of Azide Components 27
3.5 General Procedure for the Preparation of 1,4-Disubstituted Triazoles 28
4. RESULTS AND DISCUSSION **29**
5. CONCLUSION **35**
REFERENCES **37**
^{1}H NMR AND ^{13}C NMR SPECTRA **45**
CURRICULUM VITAE **57**

ABBREVIATIONS

BET : Brunauer–Emmett–Teller theory
BuOH : Buthanol
$CDCl_3$: Deuterated chloroform
CH_3CN : Acetonitrile
CuAAC : Copper(I) catalayst azide-alkyn cycloaddition reaction
$CuCl_2$: Copper (II) chloride
CuL_x : Copper-Ligand complex
DMSO : Dimethyl sulfoxide
ESI^+ : Mass spectra
EtOH : Ethanol
FTIR : Fourier transform infrared spectroscopy
^{1}H-NMR : Nuclear magnetic resonance spectroscopy
HOMO : Highest occupied molecular orbital
LUMO : Lowest unoccupied molecular orbital
MeOH : Methanol
NEt_3 : Triethylamine
PMDETA : *N, N, N',N'', N''*-Pentamethyldiethylenetriamine
XRD : X-ray diffraction patterns
SEM : Scanning electron microscopy
SECM : Scanning electrochemical microscopy
THF : Tetrahydrofuran
US/MW : Ultrasound/Microwave
UV/VIS : Ultra violet/Visible
ZnO : Zinc oxide
ZnO NPs : Zinc oxide nanoparticles

LIST OF TABLES

Page

Table 2.1 : Physical properties of ZnO 19
Table 2.2 : Synthesis methods of ZnO Nanoparticles..... 20

LIST OF FIGURES

Page

Figure 2.1 : Synthesis of 1,2,3-triazoles via 1,3-dipolar cycloaddition of azides and terminal alkynes. 5
Figure 2.2 : In-situ generation of copper(I) catalyst via electron transfer mechanisms. 6
Figure 2.3 : In-situ formation of Cu(I) via photoredox reaction 9
Figure 2.4 : Photoinduced CuAAC "click" reactions by direct (i) and indirect (ii) reduction pathways of Cu(II) to Cu(I) 9
Figure 2.5 : Selective functionalization of independently addressable electrodes with ferrocene by electro-click chemistry 12
Figure 2.6 : Reduction of Cu(II) to Cu(I) by SECM (Left) and immobilization of fluorophore onto a glass substrate 12
Figure 2.7 : Simplified representation of the proposed C–N bondmaking steps in the reaction of copper(I) acetylides with organic azides. [Cu] denotes either a single-metal center CuL_x or a di-/oligonuclear cluster Cu_xL_y 14
Figure 2.8 : Mechanism of Cu(I) azide-alkyne cycloaddition reaction 15
Figure 2.9 : The hexagonal wurtzite structure model of ZnO. The tetrahedral coordination of Zn-O is shown. O atoms are shown as larger white spheres while the Zn atoms are smaller brown spheres 19
Figure 2.10 : Shematic representation of applications of ZnO 24
Figure 4.1 : FESEM image of ZnO NPs 29
Figure 4.2 : XRD patterns of ZnO NPs 29
Figure 4.3 : UV-vis spectra of ZnO NPs. 30
Figure 4.4 : Photoinduced reduction of Cu(II) species with the help of zinc oxide nanoparticles as evidenced by UV-vis measurements 31
Figure 4.5 : Kinetics of the photoinduced CuAAC using zinc oxide nanoparticles.. 32
Figure 4.6 : Visible light-induced CuAAC of several of azides and alkynes using zinc oxide nanoparticles as photocatalyst 33

VISIBLE LIGHT-INDUCED COPPER(I)-CATALYZED AZIDE ALKYNE CYCLOADDITION WITH ZINC OXIDE SEMICONDUCTOR NANOPARTICLES

SUMMARY

In the past decade, selectivity, efficiency and diversity are the most important and required subjects for various reaction systems. “Click chemistry” can be given as an example for these systems offering remarkable advantages. Copper(I)-catalyzed azide–alkyne cycloaddition (CuAAC) reactions between azides and terminal alkynes which developed by the groups of Sharpless and Meldal, have become the most popular click reactions to date. These reactions are versatile, regiospecific, and exhibit a high efficiency under mild reaction conditions with little or no by-products. Although there are a variety of metals that can be used as a catalyst for the azide-alkyne cycloaddition reactions, copper stands out as the only metal for the reliable, simple, fast and 1,4-regiospecific catalysis. With all these excellent features, CuAAC has found precious applications in different fields such as drug discovery, biochemistry, polymer chemistry and materials science.
Recently, there is an explosive growth of research in the field of nanomaterials due to their operation for materials and devices using different techniques at nanometer scale. Nanoparticles are a part of nanomaterials that are defined as a single particles 1–100 nm in diameter and they have been a common material to develop new cutting-edge applications in communications, energy storage, optics, transmission, environmental protection, cosmetics, biology, and medicine due to their attractive optical, electrical, and magnetic properties. Moreover, nanoparticles can be combined with a wide range of metals and semiconductor core materials that bring in advantageous properties such as fluorescence and magnetic treatment. Amongs all the various types, zinc oxide - semiconductor metal oxide nanoparticles- are the most preferred type with their own importance due to their vast area of applications, such as, gas sensor, chemical sensor, bio-sensor, cosmetics, storage, optical and electrical devices, solar cells, and drug-delivery.

In this thesis, a visible light-induced copper(I)-catalyzed azide-alkyne cycloaddition (CuAAC) strategy is carried out benefiting from the electron transfer reactions of zinc oxide nanoparticles (ZnO NPs) to achieve the required catalyst for the coupling process. Semiconductor ZnO NPs as a heterogeneous photocatalyst releases electrons on UV/VIS irradiation resuting in the photoreduction of air-stable copper(II) ions to copper(I) which is the catalyst of the CuAAC reaction A variety of azide and alkyne components has been examined and the system tolerates different substrates in the click reaction well. ^{1}H-NMR and FTIR spectroscopy are used for the characterization of the reactions and it was determined that a triazole forms with the consumption of the starting azide and alkyne molecules.

ZnO YARI-İLETKEN NANOPARTİKÜLLERİ KULLANILARAK HETEROJEN FOTOKATALİZ SİSTEMİ İLE AZİD-ALKİN ÇIT-ÇIT REAKSİYONU

ÖZET

Geçtiğimiz son on yılda, ideal sentezin üç kriteri olan etkinlik, çeşitlilik ve seçicilik özelliklerini karşılayan reaksiyon sistemlerine olan ilgi hızla artmıştır. Günümüzde bu kriterleri yerine getiren en popüler reaksiyonlar "çıt-çıt" reaksiyonları olarak bilinmektedir. ''Çıt-çıt'' kimyası terimi ilk kez 2001 senesinde Sharpless ve arkadaşları tarafından ortaya koyulmuştur. Bunu takip eden senelerde önemi anlaşılmış ve konu üzerine birçok çalışma yapılmıştır. Çıt-çıt kimyası ürünleri kararlı olan, sentez koşullarında hava, su ve çözücü kirliliklerinden etkilenmeyen, yüksek verimli, hızlı, yüksek seçicilikli, birçok fonksiyonel grupla uyumlu, ihmal edilebilir seviyede yan ürün oluşturan yada yan ürün vermeyen ve gerektiğinde, kromatografik olmayan kristalizasyon veya destilasyon gibi fiziksel saflaştırma yöntemlerinin yeterli olduğu kimyasal tepkimelerden oluşmaktadır. Sahip olduğu etkin özellikleri sayesinde, Çıt-çıt kimyası olarak adlandırılan bu geniş reaksiyon sınıfı polimer teknolojisinde bir araya getirilmesi çok zor görünen grupların kolaylıkla birleştirilmesini sağlamaktadır.

Çıt-çıt reaksiyonları genel olarak dört ana grupta toplanmaktadır. Azid ve alkin gruplarının Huisgen 1,3-dipolar halkakatılma reaksiyonu başta olmak üzere; epoksit, aziridin ve aziridinyum gibi küçük üyeli halkaların nükleofilik halka açılma tepkimeleri, Diels-Alder (DA) tepkimeleri ve tiyol fonksiyonel grubu ile bir çifte bağ arasında meydana gelen tiyol-en tepkimesi de çıt-çıt kimyası olarak sınıflandırılmıştır.

Huisgen 1,3-dipolar siklokatılma reaksiyonu, azid ve alkin gruplarını birleştiren önemli bir reaksiyondur. Ancak bu tepkime yüksek sıcaklıkta, düşük seçicilikte ve uzun sürede gerçekleşmektedir. Sharpless ve Meldal bu reaksiyonu basit reaksiyon koşullarında, yüksek verimle, düşük termodinamik entalpilerde yüksek hassasiyete ulaşarak, kısa sürede gerçekleştirerek bakır katalizörünün çıt-çıt reaksiyonları için olan önemini ortaya koymuştur. Katalizör olmadan gerçekleştirilen tepkimeler ek ısıya ve uzun sürelere ihtiyaç duymaktadır. Bakır katalizörlüğünde ise oda koşullarında kolaylıkla gerçekleştirilebilen bir tepkime olup, fazladan bir ısı uygulaması gerektirmez ve geniş bir sıcaklık aralığında kısa sürede gerçekleşebilir. Tepkime katalizörsüz gerçekleştirildiğinde reaksiyon etkinliği ortalama 10^7 kat düşmektedir. Ayrıca katalizörsüz gerçekleştirilen reaksiyonda yan ürün olarak 1,5-disübstitüye triazolü oluşmaktadır. Bu durum çıt-çıt kimyasının oluşan ürün kromotografik yöntemlere başvurmaksızın ayrılabilir ilkesinin gereğini de sağlamamaktadır. Bu özelliklerinden dolayı bakır katalizörlü azid-alkin halkakatılma reaksiyonu (CuAAC) en çok kullanılan çıt-çıt reaksiyonu haline gelmiştir ve organik kimya, supramoleküler kimya, ilaç kimyası, biyokonjugasyon ve malzeme bilimi gibi birçok uygulama alanında önemli bir yere sahiptir.

Çıt-çıt reaksiyonlarının bu kadar geniş alanlarda kullanılması katalizör çeşitliliğini de beraberinde getirmektedir. Sistemde farklı reaksiyonlar için çeşitli metal katalizörlerinin (Ru,Ni,Pt,Pd ve Cu(I)) kullanılması mümkündür. Fakat bu metal katalizör çeşitliliği içerisinde en çok tercih edilen katalizör Cu(I) ve türevleridir. Bakır türevi katalizörlerin kullanıldığı sistemlerde verim %90-95 civarlarında olmaktadır. Bakır katalizörlü azid-alkin 1,3-dipolar halka katılma tepkimesi olarak bilinen çıt-çıt tepkimesi bakırın yükseltgenme ve indirgenme olaylarına dayanmaktadır. Sentezler sırasında Cu(I) elde etmek için uygun indirgenme ajanları yardımıyla gerek kimyasal ve elektrokimyasal yöntemler gerek fotokimyasal yöntemler kullanmak mümkündür. Fotokimyasal tepkimeler ısıyla gerçekleşen tepkimelere göre, daha düşük enerji ihtiyacı, hızlı gerçekleştirilebilme ve hem konum hem de zaman olarak kontrol edilebilme özelliklerinden dolayı önemli avantajlara sahiptirler. Son zamanlarda fotouyarılmış 1,3-dipolar halkakatılması, fotouyarılmış tiyol-en ve tiyol-in, fotouyarılmış gerilmiş halkalı alkin ve azidlerin siklokatılması, fotouyarılmış benzodioksinon ve alkollerden ester oluşumu ve fotokimyasal diels-alder tepkimeleri foto çıt-çıt tepkimeri olarak geliştirilmiştir.

Bakır elementi +2, +1 ve 0 olmak üzere üç farklı oksidasyon basamığına sahiptir. Termodinamik olarak en kararlı olan olan Cu(I) iyonudur. Cu(I) iyonu elektron vererek Cu(II) iyonuna yükseltgendiği gibi orantısız parçalanarak Cu(II) ve Cu(0) iyonlarına dönüşebilmektedir. Cu(I) iyonları oksijen varlığında Cu(II) ye yükseltgendiği için tepkime koşullarında ortamdan oksijenin uzaklaştırılması gerekmektedir. Bu dezavantaj oksijenden etkilenmeyen Cu(II) iyonunun tepkime sırasında kimyasal, fotokimyasal yada elektrik akımıyla indirgenmesiyle elde edilen Cu(I) iyonu katalizör olarak kullanılarak giderilmiştir.

İdeal sentez için oluşturulmaya çalışılan elverişli koşullar, geliştirilen yeni kimyasal yöntemler dışında kullanılan yeni teknoloji materyaller de desteklenmektedir. Bu amaçla, çeşitli teknikler kullanılarak nano boyutlu yeni materyaller üretilmektedir. Nanomateryaller, boyut ve şekillerine bağlı olarak farklı özelliklere sahip olan metaller, yarı iletkenler, metal oksitler ve organik ya da biyomateryaller olabilirler. Nanoboyutlu malzeme olarak tanımlanan yapılar; nanokristaller, nanopartiküller, nanotüpler, nanoteller, nanoçubuklar veya nano ince filmler gibi farklı sınıflara ayrılmaktadır.

Nanotanecikler, her birinin boyutu 1-100 nanometre (nm) arasında olan hacimsel yapılı malzemelerden çok farklı ve üstün özellikler sergileyen taneciklerdir. Nanotanecikler gösterdikleri üstün özellikler sayesinde elektrik-elektronik, biyomedikal, otomotiv ve kimya sektörleri başka olmak üzere birçok endüstriyel alanda kullanıma sahiptirler. Nanotaneciklerin fizikokimyasal ve morfolojik özelliklerinin kullanılan başlangıç malzemesinin özelliğinden etkilenmesinden dolayı farklı üretim yöntemlerin geliştirildiği görülmektedir. Nanotanecik özelliklerinin çekiciliğinin günümüzde bilinen nedenleri ise; kuantum boyut etkileri, elektronik yapısının boyut bağımlılığı, yüzey atomlarının benzersiz karakterleri ve yüksek yüzey/hacim oranı olarak ön plana çıkmaktadır. Nanotanecik sentezi bu yapıların sergiledikleri olağandışı özellikler sebebiyle yüksek aktiviteli katalizörler, optik uygulamalar için özel teknolojik malzemeler ile birlikte süperiletkenler, aşınmaya karşı katkılar, yüzey aktif maddeler, ilaç taşıyıcılar ve özel teşhis aletleri gibi birçok teknolojik ve farmakolojik ürünlerin hazırlanmasının yolunu açmıştır. Bunların yanı sıra, malzemelerin nanoboyut seviyesinde kontrolü nanotaşıyıcılar, sensörler, nanomakinalar ve yüksek yoğunluklu veri depolama hücreleri gibi kendine özgü işlevselliğe sahip minyatürleştirilmiş aygıtların gerçekleştirilmesine izin vermektedir.

Çinko oksit var olan yarı iletken nanotanecikler arasında öne çıkan çok yönlü bir materyaldir ve tercih edilmesinin en önemli sebebi kimya, kozmetik, ilaç salınımı, güneş pilleri, biyosensörler, optic ve elektronik malzemelr gibi pek çok alanda uygulanabilir olmasıdır. Çinko oksit yarı iletken nanotanecikleri ışığa karşı yüksek duyarlılığa sahiptirler ve foto uyarılma ile ortama serbest elektronlar vererek ışık altında redoks reaksiyonlarının gerçekleşmesini sağlarlar.

Bu tez çalışmasında, heterojen bir fotokatalizör olan yarı iletken çinko oksit nanotaneciklerinde (ZnO NPs) oluşan elektron transfer reaksiyonlarından yararlanılarak gerçekleştirilen, bakır(I) azid-alkin halkakatılma (CuAAC) reaksiyonları incelenmiştir. CuAAC çıt-çıt reaksiyonunu fotokimyasal olarak katalizleyecek olan Cu(I) katalizörünün oluşumu, görünür ışıkla uyarılan Zn nanotaneciklerinden serbest kalan elektronların, Cu(II) iyonlarını Cu(I) iyonlarına indirgemesiyle elde edilmiştir. Çeşitli azid-alkin bileşikleri üzerinde yöntem denenerek çıt-çıt reaksiyonunun farklı fonksiyonel gruplar içeren azid ve alkin uçlu moleküllerle başarıyla gerçekleştiği görülmüştür. Deneysel sonuçlar, Nüleer Manyetik Rezonans (^{1}H-NMR) ve Fourier Dönüşüm İnfrared (FTIR) spektroskopisi ile karakterize edilmiştir. Aydınlatma öncesinde ve sonrasında ölçümler yapılmış, ^{1}H-NMR karakterizasyonunda, aydınlatma öncesinde var olmayan triazol halkasının karakteristik piki aydınlatma sonrasında elde edilen grafiklerde açıkça görülmüştür. FTIR karakterizasyonunda yapılan ölçümlerde ise aydınlatma öncesinde 2100 nm'de görülen azid pikinin aydınlatma sonrasında kaybolmasıyla ortamda var olan azid fonksiyonelitesinin alkin gruplarıyla triazol halkasını oluşturarak tükendiği belirlenmiştir.

1. INTRODUCTION

In search of ever-newer and enduring forms of energy which can be obtained, for example, by converting the inexhaustible energy of sunlight to the chemical or electrical energy, semiconductor materials have emerged as potential solution for many energetic issues.[1] Semiconductor nanoparticles which are highly sensitive towards light and undergo photoexcitation releasing charge carriers (electron-hole pairs),[2] have been reported to trigger numerous catalytic processes under light by enabling various redox reactions and are being commercialized as mediators in solar cells systems to make use of light.[3]

As heterogeneous photocatalyst, semiconductor materials have been increasingly utilized in many fields of chemistry and materials and it has been the aim of this contribution to examine the potential of semiconductor zinc oxide nanoparticles (ZnO NPs) as the photocatalyst to conduct the copper(I)-catalyzed azide-alkyne cycloaddition (CuAAC). First coined by Sharpless[4, 5] and Meldal,[6] CuAAC has been extensively investigated and applied in a wide range of applications from various areas of organic chemistry[7] and materials science and polymers[8, 9] to bioconjugation[10] and drug delivery.[11]

A great deal of efforts has gone into understanding the catalytic process of CuAAC[12] and how efficient copper catalysts can be availed of to be used in catalyzing the click reaction. In relation to this, it has been shown that light can be used as an external stimulus to generate the required CuI catalyst for CuAAC which relies on the photochemically reduction of CuII complexes.[13] CuII/ligand complexes are reduced to CuI directly by absorbing light without the use of additional photoinitiators,[14, 15] through photoexcitation of the CuII/ligand complex and following an electron transfer from the π-system of the ligand to the central ion or in an indirect manner using photoinitiators to generate radicals capable of reducing CuII.[16-21] Additionally, photosensitizers furnishing the photoinduced electron transfer reactions have also been reported as efficient photoinitiating systems. [22]

In this thesis, a visible light-induced copper(I)-catalyzed azide-alkyne cycloaddition (CuAAC) strategy is carried out benefiting from the electron transfer reactions of zinc oxide nanoparticles (ZnO NPs) to achieve the required catalyst for CuAAC. With the aid of semiconductor ZnO NPs as a heterogeneous photocatalyst, a copper(I) catalyst is formed to photochemically catalyse the click reaction as a result of the photoreduction of air-stable copper(II) ions to copper(I) by releasing electrons from the nanoparticles on irradiation. A variety of azide and alkyne components has been examined and the system tolerates different substrates in the click reaction well.

2. THEROTICAL PART

2.1 Click Chemistry

Since the birth of modern chemistry, chemists have tried to develop chemical reactions that include minimum work-up, maximum yields, limited side reactions and precise chemical connections. In 2001, Kolb, Finn and Sharpless introduced a novel and remarkable synthetic strategy with the aim of binding two molecular building blocks, termed "click chemistry" [13]. They defined this new approach with a set of stringent criteria that "*the reaction must be modular, wide in scope, give very high yields, generate only inoffensive by-products that can be removed by nonchromatographic methods, and be stereospecific (but not necessarily enantioselective). The required process characteristics include simple reaction conditions (ideally, the process should be insensitive to oxygen and water), readily available starting materials and reagents, the use of no solvent or a solvent that is benign (such as water) or easily removed, and simple product isolation. Purification –if require- must be by nonchromatographic methods, such as crystallization or distillation, and the product must be stable under physiological conditions.*"[23].

Click chemistry is very useful and "green" concept with all of the features that has mentioned in its definition [24]. Therefore, applications of click reactions have had a profound influence on different areas of research and thousands of scientific articles have been published since 2001 about utilization of click reactions for preparative organic synthesis, bio-conjugation, polymer and material sciences, and nanotechnology [13]. Furthermore, it is a highly selective and efficient chemical method which uses a wide scope of materials, providing the best yields and highest rates. Due to its facile and selective chemical transformations, click chemistry has recently emerged as a suitable, versatile, and reliable method for labelling various biomolecules, drug discovery, clinical medicine, combinatorial chemistry, and DNA research [25].

The most commonly employed click reactions that have been adapted to fulfill these criteria are:

i. cycloaddition reactions (most commonly Huisgen 1,3-dipolar cycloaddition[26, 27], but also Diels-Alder reaction[28-31]),

ii. nucleophilic ring-opening reactions of strained heterocyclic electrophiles (epoxides, aziridines and aziridinium ions) [32],

iii. non-aldolcarbonyl chemistry (ureas, oximes and hydrazones) [33-35],

iv. additions to carbon-carbon multiple bonds (especially thiol-ene chemistry but also Michael additions) [36-40].

2.1.1 Copper(I)-catalyzed azide-alkyne cycloaddition reactions (CuAAC)

Copper(I)-catalyzed azide–alkyne cycloaddition (CuAAC) reactions between azides and terminal alkynes were developed independently by the groups of Meldal and Sharpless in 2002 and have become the most popular click reactions to date. CuAAC reaction with the unique features that make it facile, versatile, regiospecific, and high efficiency under mild reaction conditions with little or no by-products represents an excellent example of the benefits from using transition metal catalysis in synthetic organic chemistry [13, 41].

The non-catalyzed (thermal) azide/alkyne reaction was discovered by A. Michael and it has been known since he reported the first synthesis of 1,2,3-triazoles from diethyl acetylenedicarboxylate and phenyl azide in 1893. After Huisgen and coworkers' thoroughly investigations of the family of 1,3-dipolar cycloaddition reaction in the middle of the 20th century, it is known as the Huisgen reaction. Although the reaction is highly exothermic (ΔH^0 between 50 and 65 kcal mol^{-1}), its high activation barrier (approximately 25 kcal mol-1 for methyl azide and propyne) results in exceedingly low reaction rates for unactivated reactants even at elevated temperature. Furthermore, since the differences in HOMO–LUMO energy levels for both azides and alkynes are of similar magnitude, both dipole-HOMO- and dipole-LUMO-controlled pathways operate in these cycloadditions [42]. Consequently, the uncatalysed Huisgen 1,3-dipolar cycloaddition reaction is a slow, high temperature, unselective process which produces an equimolar mixture of 1,4- and 1,5-disubstituted 1,2,3-triazole regioisomers (Figure 2.1A) [41]. Under these conditions azide–alkyne cycloaddition reactions was not useful in the click context, and its potential was not revealed until the discovery of the reliable and broadly useful catalysis by copper(I) [42]. On the other hand, in the presence of catalytic copper(I)

species as a catalyst the reaction is accelerated in a remarkable way and the reaction rate may increase up to 7 orders of magnitude higher than that of the uncatalysed process [43]. Moreover, a striking improvement of the regioselectivity is observed, with 1,4-disubstituted isomer being the only product formed (Figure 2.1B) [41]. The reaction is not importantly affected by the steric and electronic properties of the groups attached to the azide and alkyne centers, and primary, secondary, and even tertiary, electron-deficient and electron-rich, aliphatic, aromatic, and heteroaromatic azides usually react well with diversely substituted terminal alkynes [42].

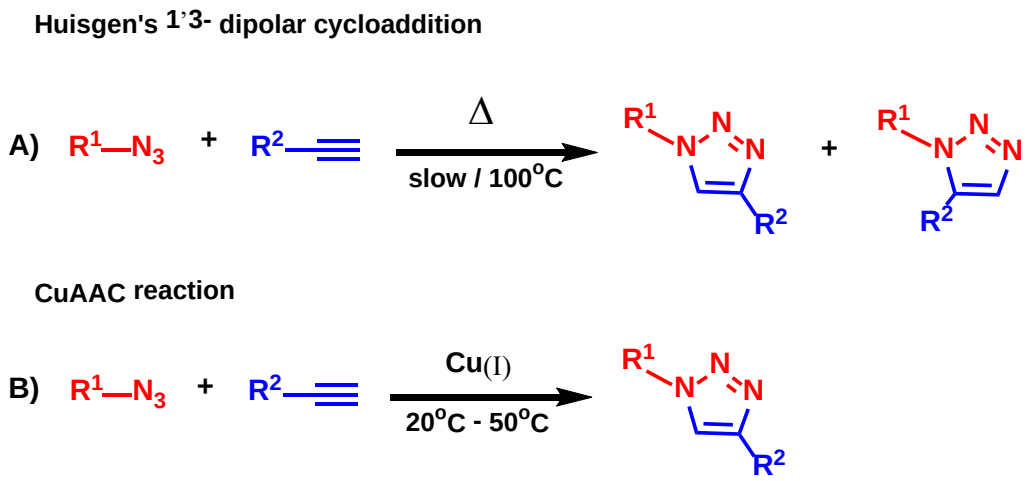

Figure 2.1 : Synthesis of 1,2,3-triazoles via 1,3-dipolar cycloaddition of azides and terminal alkynes.

Therefore, the CuAAC process has emerged as the most prominent example of "click" chemistry, and more than a thousand research articles have been published by scientists from different disciplines on CuAAC since 2002. The reasons for its extraordinary success are that this transformation is high yields, easy to perform and widely practicable [24]. Although, 1,2,3-triazole heterocycle does not occur naturally, synthetic molecules including the 1,2,3-triazole core show interesting biological properties [44]. Furthermore, the 1,2,3-triazole has advantageous features about chemical stability that it is inert against oxidation, reduction and hydrolysis under acidic or basic conditions even at high temperature making it a perfect mimetic of the amide bond [11]. It can attend in hydrogen bond formation and in dipole–dipole interactions. As a consequent of that, the CuAAC has found precious applications in different fields such as drug discovery, biochemistry, dendrimer and polymer chemistry and materials science [41].

Up to now, copper stands out as the only metal for the reliable, simple, and 1,4-regiospecific catalysis of the azide–alkyne cycloaddition. Actually, other metals known to catalyze various transformations of alkynes have not so far yielded effective catalysts for the conversion of azides and terminal alkynes to 1,4-triazoles [42]. Formation of the 1,5-disubstituted triazole isomer from azides and terminal alkynes upon catalysis by ruthenium cyclopentadienyl complexes (RuAAC reaction) has examined by the group of Fokin and Sharpless and reported in 2005 [45], Ni^{2+} [46], Pd^{2+} [47], Pt^{2+} [47] and Au^{I} [48] metals can be described other less efficient catalysts.

2.1.1.1 The catalytic system

A large variety of copper source can be used for the CuAAC reaction provided that catalytically active Cu(I) species are formed in the reaction medium. It is essential to keep the Cu(I) concentration at its maximum in order to make easy the reaction. There are several methods are available for formation of the Cu(I) catalyst required for CuAAC reactions which include the in situ reduction of Cu(II) to Cu(I) by 1) various reducing agents, [49] 2) photochemical, [16] 3) electrochemical [50] redox processes 4) copper-containing nanoparticles [51, 52].

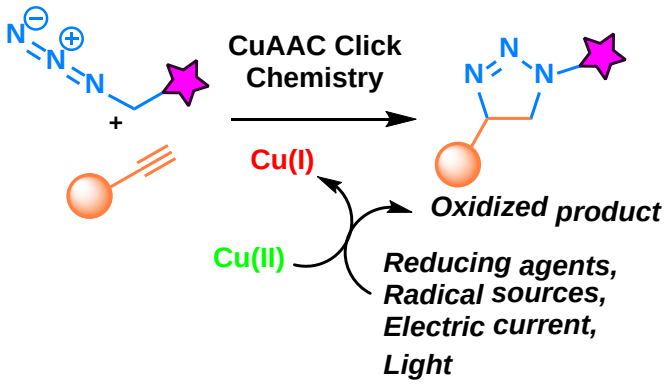

Figure 2.2 : In-situ generation of copper(I) catalyst via electron transfer mechanisms. [13]

(i) Reducing agents

In-situ reduction of Cu(II) salts is a suitable method to produce Cu(I) for the CuAAC click reaction. Cu(II) salts may readily be reduced to the catalytically active Cu(I) species in the CuAAC process by reducing agents such as alcohols, amines, aldehydes, thiols, phenols, and carboxylic acids. Most frequently used reducing agents are ascorbic acid, sodium ascorbate, quinone, hydroquinone, vitamin Kl,

glutathione and cysteine. Furthermore, metals can be employed as reducing agents to maintain the oxidation state of the Cu (I) catalyst or of other metal catalysts. Metallic reducing agents include, but are not limited to, Cu, Al, Be, Co, Cr, Fe, Mg, Mn, Ni, and Zn. Among these reagents, ascorbate is a mild and cheap one and its combination with a Cu(II) salts such as $Cu(II)SO_4.6H_2O$ or $Cu(OAc)_2.H_2O$, has been approved as common method for the CuAAC [53]. The most widely applied conditions to generate Cu(I) species in solution contains the in situ reduction of $CuSO_4 \cdot 5H_2O$ with sodium ascorbate (3–10 fold-excess) in water/alcohol (MeOH, EtOH or BuOH) mixtures, reported by the Fokin and Sharpless group in 2002. The major advantage of this protocol resides in being compatible both with oxygen and water. The presence of an organic co-solvent (alcohol or DMSO) ensures the solubility of more hydrophobic reactants. The aqueous compatibility of this method is very useful for the application of CuAAC in bioconjugation as well as for organic syntheses [24, 41].

(ii) Photochemical reducing

Photochemical control is a non-invasive process in which the amplitude, wavelength, spatial location, and timing of the light illumination can be easily controlled.[49, 54, 55] Photochemical reactions include the absorption of light to generate excited molecules with high reactivity, which then undergo chemical changes. Unimolecular reactions [56, 57], like ionization, dissociation, and isomerization reactions, as well as bimolecular reactions [58, 59] such as cycloaddition and intermolecular electron transfer, can be given as examples for light activated reactions [14].

Photochemical reactions can also be spatially and temporally controlled by focusing photons onto a given area, unlike thermally initiated reactions and this level of control is not probable with conventional thermal reactions [13]. Wavelength, light intensity, exposure time and scan speed can be controlled for the desired materials, as needed.[12] Temporal control of the processes based on photoinduced systems relies on the simplicity of being able to switch on/off a light source. In this way, the control of the freedom on the process is high when compared to thermally driven reactions that require heating and cooling periods. In contrast, thermally driven reactions have inevitable retardation in reaching the desired temperature and thus equilibrium. Also, during heating process there is a gradual temperature ramp passing through gradient

energy levels which may be available to initiate side-reactions and of course yield undesired products. This is also possible for the cooling down period since the temperature will not revert to ambient temperature instantly, again, the system would go through a level of energy available to trigger the possible side reactions.

Photoinduced click reactions not only combine effectively the classical benefits of click chemistry but also have a lot of additional advantages of the photochemical process. For instance, these reactions can be activated at a specific time and location, resulting in a powerful method for chemical synthesis, tailored material fabrication, and biorthogonal conjugation [13].

Photoinduced cycloaddition reactions involving CuAAC, Diels-Alder and tetrazole-alkene supply a unique means for enabling the spatial and temporal control over chemical and biological processes. Among all click reactions, CuAAC is the first one to set the standard for click reactions and also, it is the most outstanding and beneficial one to utilize in material science. The first example of photoinduced CuAAC, was reported by König and Ritter in 2006. The process was driven by in-situ generated Cu(I) catalyst from Cu(II) species using a redox-active riboflavin tetraacetate as a chromophore and an electron donor.[16] In that communication, riboflavin tetraacetate was photoreduced to flavin in the presence of an electron donor such as benzyl alcohol or trimethylamine. After that, the reduced chromophore converted Cu(II) to Cu(I) that catalyzed cycloaddition of benzyl azide and phenyl acetylene under anaerobic conditions (Figure 2.3). The light effect on the CuAAC reaction is further studied by carrying out periodical light on/off switching studies. The reaction mixture is exposed to light for 90 minutes affording approximately 7% conversion. Thereafter, the light source is switched-off systematically and the rate of cycloaddition reaction decreased during the dark periods. The rate reduction of the CuAAC reaction in dark periods may be due to the instability of the active Cu(I) catalyst in aqueous solutions in the absence of any stabilizing ligands and disproportionates. Re-exposure of light for the second run promotes the CuAAC process, and kinetics of the system reaches up to the first run level.

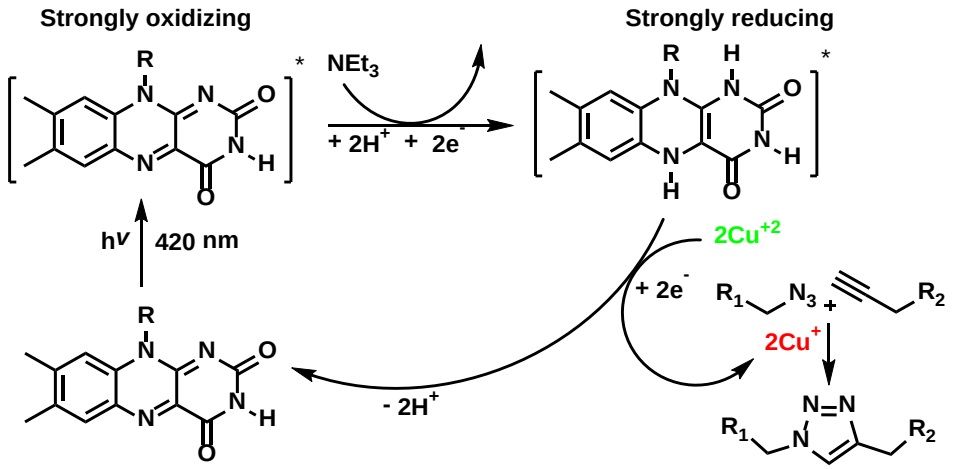

Figure 2.3 : In-situ formation of Cu(I) via photoredox reaction

In 2010, Yagci et al.[14, 18] and Bowman et al.[51] have developed a novel photoreductive strategy for the in-situ generation of catalytically active Cu (I) complexes from inactive Cu(II) complexes to catalyze CuAAC reaction between azides and alkynes. (Figure 2.4). In direct system, the in-situ generation of the Cu (I) can be performed by the photoreduction of specific Cu(II) complexes via ligand metal charge transfer. In indirect approach, a variety of radical generator like photoinitiator absorbs light in the UV-visible region where the copper complex is colorless, and forms reactive intermediates, such as free radicals or carbocations that promote the photoreduction of Cu(II) to Cu(I) [13].

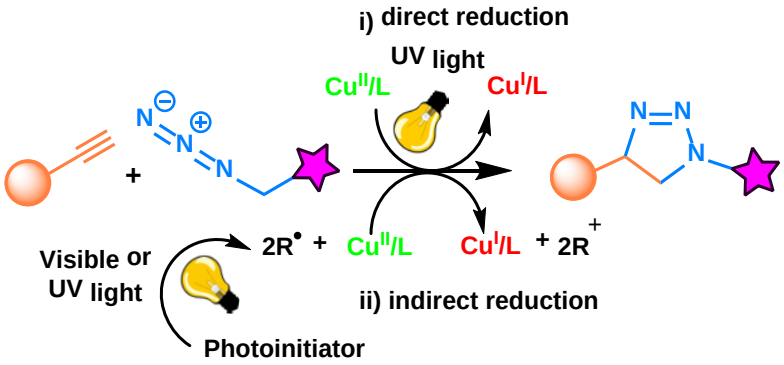

Figure 2.4 : Photoinduced CuAAC "click" reactions by direct (i) and indirect (ii) reduction pathways of Cu(II) to Cu(I)

A photosensitive CuAAC catalytic system formed by an air-stable $CuCl_2$/PMDETA complex upon UV/VIS light irradiation which results in the formation of Cu(I) species, in direct method. Cycloaddition reactions were carried out under aerobic conditions and reached completion with continuous irradiation for 2–3 h.[14] This method has been shown to implement the CuAAC transformation of phenyl azide

with various terminal alkynes, phenyl acetylene, propargyl acrylate, propargyl alcohol and propargyl bromide, in desirable yield and purity.

In direct photolysis, the strong absorption at UV region triggers an intramolecular electron transfer from the π-system of the ligand towards the metal ion, resulting in the reduction of Cu(II) to Cu(I) ion, and oxidation of the ligand into a radical complex.[60] Furthermore, the stability of Cu(I) complex after the photolysis is a significant issue that should be emphasized. When the Cu(II)-amine complex is shown to promote ligand–metal-charge transfer and the CuAAC reaction at the same time, the Cu(I) ions are stabilized by the amines. The aliphatic amine ligands not only use to provide an electron to reduce Cu(II) upon irradiation, but they also serve to stabilize Cu(I) ions, once formed. Also, importantly, they increase the solubility of the Cu(II) in most organic solvents. Type of ligands plays a crucial role in controlling the efficiency and effectiveness of the photoinitiated CuAAC reaction. Among the aliphatic primary, secondary and tertiary amines, the tertiary amines such as triethylamine, tetramethylethylenediamine, PMDETA and hexamethylenetetramine are reported the most effective ligands for the CuAAC. The reaction kinetics are also accelerated by increasing the tertiary amine ligand concentration with a ratio of ligand to Cu(II) of 4:1 yielding the maximum conversion in the shortest time.[19]

The indirect activation of the CuAAC reaction involving electron transfer between photochemically generated electron donor radicals and Cu(II) ions appeared to be more suitable than direct photochemical reduction due to the longer absorption characteristics of the free radical photoinitiators and faster reaction rates.[18] In this system, a photoinitiator absorbs light in a spectral region where the copper complex is transparent, and forms reactive intermediates such as free radicals or carbocations. Then, these species effectively promote photoreduction of Cu(II) to Cu(I). The characteristics of the photochemically generated radicals and the redox properties of the copper complex are critical for the success of CuAAC reactions.

The cycloaddition reactions are initially investigated through FTIR, ^{1}H-NMR, and ESI^{+} mass spectroscopic analysis of the model compounds. All of these monitoring techniques confirm that a triazole is formed, and the starting azide and alkyne molecules are consumed.[13]

Photoinduced CuAAC reactions can be temporally controlled since the activating light beam can be turned on and off as desired. Besides, the overall rate of the click process can be altered by light intensity, photoinitiator concentration, and irradiation time. Detailed kinetic investigations have pointed out that Cu(I) is not rapidly consumed during the reaction in the dark stages, and it may be a result of the disproportionation of Cu(I) to Cu(II) and Cu(0), which probably cause the regeneration of Cu(I). This feature allows a reaction to be completed by using small amount of UV irradiation and copper catalyst. However, a photoinduced CuAAC reaction can be stopped at any time by simply foaming air into the reaction mixture, which leads to an irreversible oxidation of the catalyst by molecular oxygen [61]. Visually, the color of the solution turns green, meaning that photogenerated Cu(I) complexes have reoxidized to Cu(II) complexes. Interestingly, nevertheless, this inhibition process is completely reversible. For example, when the reaction mixture is purified with argon gas and then exposed to UV irradiation for 15 min, the click reaction returns at the same rate as before. These results propose that light is a strong stimulus for gaining spatial and temporal control of a CuAAC reaction.[62, 63]

(iii) Electrochemical reducing

Since the electrochemical processes control the redox state of copper which in turn activate or deactivate the catalyst over triazole formation, CuAAC click reaction can be realized by electrochemical means. The electrochemical reaction proceeds in minutes at sub-micromolar catalyst concentration and mild potentials for catalyst activation are enough. Moreover, such reactions could proceed in aqueous or mixed aqueous-organic mediums. [64]

Selective functionalization of independently addressable electrodes by electrochemical activation of the copper catalyst for triazole formation was first demonstrated by Devaraj et al (Figure 2.5).[64] Thus, a general strategy for the immobilization of functional objects onto electrodes was described. Moreover, the ability to switch on or off the reaction by electrical current with chemo-selectivity makes the approach much more attractive in material science.

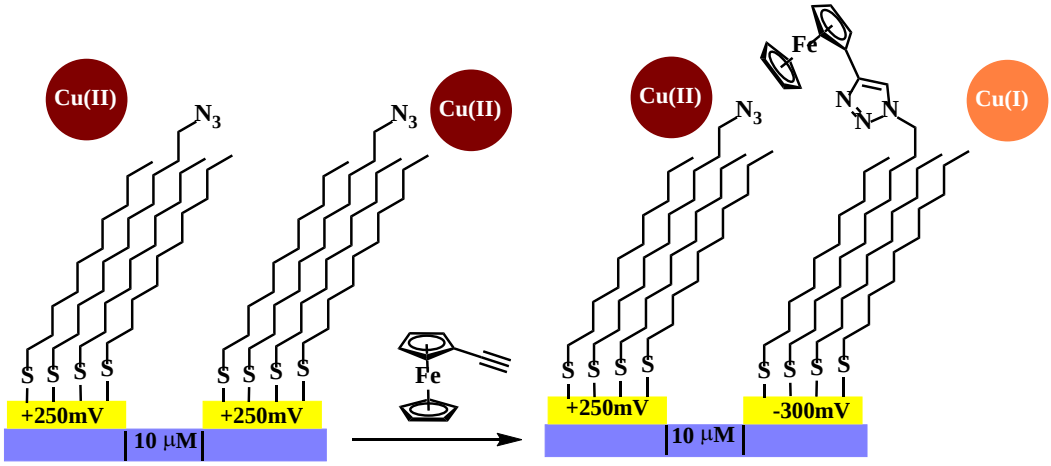

Figure 2.5 : Selective functionalization of independently addressable electrodes with ferrocene by electro-click chemistry

The same concept was modified and the click reaction was achieved directly by scanning electrochemical microscopy (SECM). SECM is a powerful tool for studying local electrochemical and chemical reactions. In this approach, the Cu(II) reduction was carried out at a SECM tip to modify a glass surface beneath.[65] As depicted in Figure 2.6, a gold microelectrode was used to reduce Cu(II) to Cu(I) locally in the small gap between the tip and the substrate to catalyze the click reaction in a small volume. Sufficient amount of Cu(I) species produced this way could catalyze the immobilization of an acetylene bonded fluorophore onto a small area of the substrate. Moreover, the tip on the small volume also prevents Cu(I) from unwanted oxidation. And the most important point of this approach is the control over the amount of deposited molecules by adjusting the tip-substrate distance, the amount of Cu(I), and the reaction time.[65]

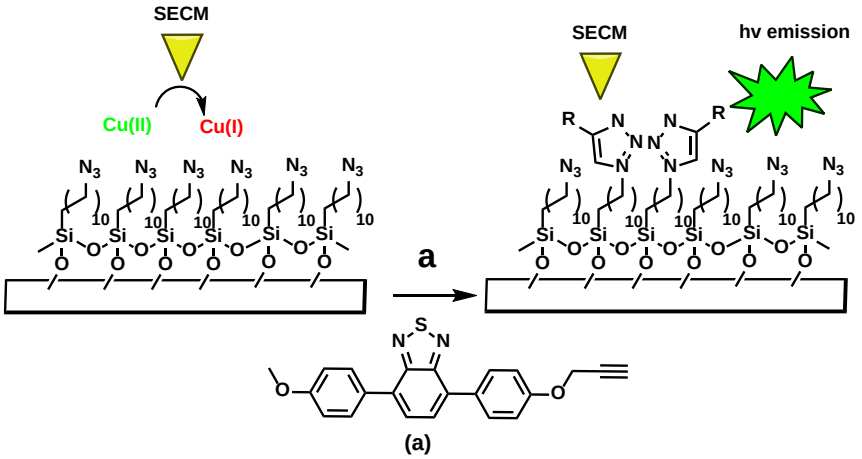

Figure 2.6 : Reduction of Cu(II) to Cu(I) by SECM (Left) and immobilization of fluorophore onto a glass substrate

(iv) Copper-containing nanoparticles

Metal nanoparticles have prominently different properties than those of the atomic or molecular system as well as those of a macroscopic solid. These properties are largely traceless to the large surface area of nanosized materials, electrodynamic interactions and the quantum size effect.[66] Generally, the benefits of using metal nanoparticles as catalysts lie on (i) the high surface-to-volume ratio of metal nanoparticles, which guarantees a large number of active sites per unit area; (ii) the enhanced reactivity, which avoids the use of ligands/additives; and (iii) the ease of separation and recyclability, which minimizes the contamination of products.[67]

The first instances about the using of Cu NPs in CuAAC were published by the groups of Orgueira[68] and Rothenberg[69] independently in 2005. In Orgueira's work, an amine hydrochloride salt was necessary to trigger the reaction by increasing the solubility of CuNPs in the reaction medium (H_2O/tBuOH). In the work reported by Rothenberg and coworkers, air stable nanometric Cu clusters stabilized by the tetraoctylammonium ion were used as catalysts for a variety of cycloaddition reactions, at room temperature, in the absence of additives.

(a) The use of Cu(I) salts

The another well-established catalytic process for CuAAC reactions is the direct use of a Cu(I) salt without a reducing agent. This procedure requires an inert atmosphere to prevent oxidation of Cu(I) to Cu(II) and the reaction result improves in an organic solvent such as CH_3CN, THF or toluene, among others. An excess of nitrogen base is necessary to facilitate the deprotonation of the alkyne to form the reactive Cu(I)-acetylide complex.[26] Moreover, the base helps to stabilize the active Cu(I) species towards oxidation or disproportionation. However, the presence of the base diminishes the yield by promoting both alkyne and triazole homocoupling. [6, 26, 70, 71] Triethylamine (TEA) and N,N,N′,N″,N″ pentamethyldiethylenetriamine PMDETA can give usual examples that are used nitrogene bases as additives in CuAAC reactions. CuBr in combination with the base PMDETA has been commonly used in applications of CuAAC in polymer chemistry.[72]

(b) The use of (Cu0) metallic copper

CuAAC reactions may also be catalyzed by Cu(I) species provided from metallic copper by simply adding a small piece of copper wire or turning into the reaction mixture. However, this method is required higher catalyst loadings and extended reactions times (up to 24 h) for completions as compared to the typical Cu_2SO_4/ascorbate or Cu(I) salts system.[6, 73] The reactions time can be notably decreased from hours to minutes by applying microwave radiation.[73] In addition, the main advantage of this protocol is the lower level of copper contamination in the products. Cravotto and co-workers reported that ultrasound (US) or simultaneous US/MW irradiation produced a significant enhancement of the cycloaddition of phenylacetylene and benzylazide in the presence of copper fine turnings or wires.[74, 75]

2.1.1.2 Mechanism

Copper catalysts drastically change the CuAAC mechanism and the outcome of the reaction, converting it to a sequence of discreet steps culminating in the formation of a 5-triazolyl copper intermediate (Figure 2.7). The key C–N bond-forming event takes place between the nucleophilic, vinylidene-like b-carbon of copper(I) acetylide and the electrophilic terminal nitrogen of the coordinated organic azide.[42]

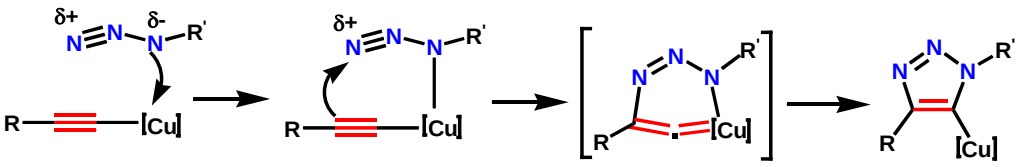

Figure 2.7 : Simplified representation of the proposed C–N bondmaking steps in the reaction of copper(I) acetylides with organic azides. [Cu] denotes either a single-metal center CuL_x or a di-/oligonuclear cluster Cu_xL_y

The initial computational treatment of CuAAC focused on the possible reaction pathways available to mononuclear copper(I) acetylides and organic azides; propyne and methyl azide were chosen for simplicity (Figure 2.8). Formation of copper(I) acetylide 2 (step A) was calculated to be exothermic by 11.7 kcal mol^{-1}, consistent with the well-known facility of this step which probably occurs through a p-alkyne copper complex intermediate. p-Coordination of alkyne to copper significantly acidifies terminal hydrogen of the alkyne, bringing it into the proper range to be deprotonated in an aqueous medium and resulting in the formation of a s-acetylide. The azide is then activated by coordination to copper (step B), forming intermediate

3. This ligand exchange step is nearly thermoneutral computationally (2.0 kcal mol^{-1} uphill when L is water), and the coordination event is synergistic for both reactive partners: coordination of the azide reveals the b-nucleophilic, vinylidene-like properties of the acetylide, whereas the azide's terminus becomes even more electrophilic. In the next step (C), the first C–N bond-forming event takes place, and a strained copper metallacycle 4 forms. This step is endothermic by 12.6 kcal mol^{-1} with a calculated barrier of 18.7 kcal mol^{-1}, which corresponds roughly to the observed rate increase and is considerably lower than the barrier for the uncatalyzed reaction (approximately 26.0 kcal mol^{-1}), thus accounting for the observed rate acceleration accomplished by Cu(I). The formation of copper triazolide is very facile and energetically favorable. When protected by steric bulk, Cu–triazolyl complexes can be isolated from CuAAC reactions,[76] and in rare cases of low catalyst loading and high catalytic rate, step E can be turnover-limiting. Alternative pathways, including the concerted cycloaddition of azide and copper acetylide, were ruled out. The coordination of the azide to copper via the terminal nitrogen, proposed in a recent review article by Meldal and Tornøe,[77] had been also examined and found to be energetically unfavorable (no feasible intermediates could be identified). There is no experimental evidence to support this proposal either.[42]

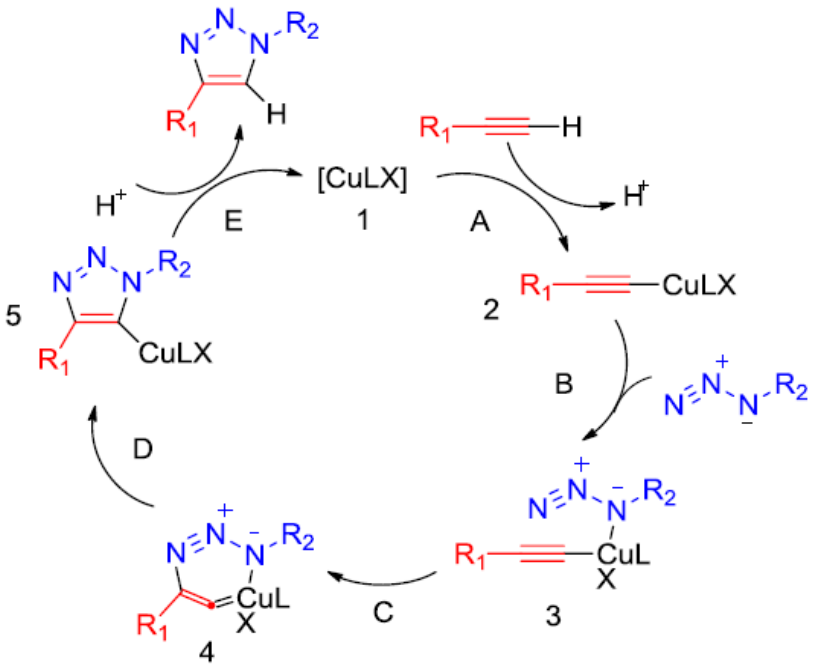

Figure 2.8 : Mechanism of Cu(I) azide-alkyne cycloaddition reaction

2.2 Nanomaterials And Zinc Oxide Nanoparticles

2.2.1 Properties of nanomaterials

Nowadays, nanotechnology is employing in assorted fields of science by its operation for materials and devices using different techniques at nanometer scale and there is an explosive growth of research in the field of nanomaterials. Nanomaterials can have different shapes and properties that may change depending on their size and/or shape. These materials may be metals, semiconductors, metal oxides, organic materials or biomaterials, hence, there is an enormous scope to design new materials with extraordinary properties.[78, 79]

Nanoparticles are a part of nanomaterials that are defined as a single particles 1–100 nm in diameter and one can reduce the dimension in one, two or all three directions to obtain thin films, wires or dots, respectively. [78, 79] For last few years, nanoparticles have been a common material to develop new cutting-edge applications in communications, energy storage, sensing, data storage, optics, transmission, environmental protection, cosmetics, biology, and medicine due to their attractive optical, electrical, and magnetic properties.[80]

Moreover, nanoparticles can be combined with a wide range of metals and semiconductor core materials that bring in advantageous properties such as fluorescence and magnetic treatment.[81] Besides, unlike their bulk counterparts, nanoparticles have reduced size associated with high surface/volume ratios that increase as the nanoparticle size decreases. As the particle size decreases to some extent, a great number of constituting atoms can be found around the surface of the particles, which makes the particles highly reactive with prominent physical properties.[82, 83]

Synthesis of nanoparticles having uniform shape and size via easy synthetic routes is the main issue in nanoparticle growth. For the past decade, scientists have been included in the development of new synthetic methods that can make enable the exact control of the morphology and size of the nanoparticles. Furthermore, nanoparticle synthesis can carry out via liquid (chemical method), solid, and gaseous media but chemical methods are the most popular due to their low cost, reliability, and environmentally friendly synthetic routes, and this method provides extremely exhaustive and accurate control of the size and shape of the nanoparticles. Generally,

nanoparticles with high surface/volume ratio are needed, but the agglomeration of small particles precipitated in the solution is the main concern in the absence of any stabilizer. In this case, stable colloid preparation is significant for nanoparticle growth. Besides, nanoparticles are generally stabilized by steric repulsion between particles due to the presence of surfactant, polymer molecules, or any organic molecules bound to the surface of nanoparticles. Occasionally Van der Waals repulsion (electrostatic repulsion) also plays important role in nanoparticles stabilization. [79]

There are various types of nanoparticles that their synthesis is related with all these issues, reported in the literature, e.g., metal nanoparticles, metal oxide nanoparticles, and polymer nanoparticles. Amongst all the various types, semiconductor metal oxide nanoparticles stand out as one of the most versatile materials, due to their different properties and functionalities. Zinc oxide (ZnO) nanoparticles are the most preferred type which have their own importance due to their vast area of applications, e.g., gas sensor, chemical sensor, bio-sensor, cosmetics, storage, optical and electrical devices, window materials for displays, solar cells, and drug-delivery.[84, 85]

2.2.2 Zinc oxide nanoparticles (ZnO NPs)

Zinc oxide nanoparticles can be called a multifunctional material owing to its unique physical and chemical properties, such as high chemical stability, high electrochemical coupling coefficient, broad range of radiation absorption and high photostability [86]. In materials science, zinc oxide is categorized as a semiconductor in group II-VI, whose covalence is on the limit between ionic and covalent semiconductors. ZnO is also an attractive material for short-wavelength optoelectronic applications with its wide energy band gap (3.37 eV), high bond energy (60 meV), large bond strength and high thermal and mechanical stability at room temperature. These properties make it suitable for potential use in electronics, optoelectronics and laser technology.[87, 88] Furthermore, ZnO can be used as a sensor, converter, energy generator and photocatalyst in hydrogen production thanks to its piezo- and pyroelectric properties [89, 90]. The hardness, rigidity and piezoelectric constant of ZnO mean that it is an important material in the ceramics

industry. Moreover, its low toxicity, biocompatibility and biodegradability make it an outstanding material for biomedicine and in pro-ecological systems. [91, 92].

Zinc oxide has a wide morphological diversity in nanostructures and this means that it can be classified among novel materials with potential applications in many fields of nanotechnology [93]. ZnO can be formed in one- (1D), two- (2D), and three-dimensional (3D) structures. One-dimensional structures compose the largest group, containing nanorods [94, 95], -needles [96], -helixes, -springs and -rings [97], -ribbons [98], -tubes [99, 100], -belts [101], -wires [102] and -combs [103]. Zinc oxide can be obtained in 2D structures, such as nanoplate/nanosheet and nanopellets [104]. Illustrations of 3D structures of zinc oxide involve flower, dandelion, snowflakes, coniferous urchin-like, etc. [105, 106]. When considering all these aforementioned structure and application features, ZnO is one of most important, beneficial and efficient substance among all known materials [93].

2.2.3 Crystal structure of zinc oxide

Actually, zinc oxide crystallizes has two main forms, hexagonal wurtzite and cubic zinc blende but the (B4 type) wurtzite structure is only obtained at optimum pressure and temperature.[107, 108] The ZnO wurtzite structure has a hexagonal unit cell with two lattice parameters, a and c, and belongs to the space group of C^4_{6V} or $P6_3mc$. The lattice parameters of the hexagonal unit cells mostly range from 3.2475 to 3.2501 Å for a and from 5.2042 to 5.2075 Å for c [109, 110] The density of the ZnO is 5.606 g/cm^3. Figure 2.9 clearly shows that one zinc atom is tetrahedrally coordinated with four oxygen atoms. Such tetrahedral coordination of ZnO gives rise to the noncentrosymmetric structure which is attributed to the piezoelectric nature that is an important property for the fabrication of microelectromechanical systems (MEMS) coupled with sensors, actuators and transducers. Due to the noncentrosymmetric behavior, it also exhibits two polar surfaces on opposite sides and each terminates with the one type of ions only [111, 112]

When the bonds along the c-direction are from cation (Zn) to anion (O) the polarity is referred to be as Zn polarity, while when the bonds along the c-direction are from anion (O) to the cation (Zn) the polarity is referred to be as oxygen polarity. This polarity is also responsible for a number of properties of ZnO, such as spontaneous

polarization and piezoelectricity, and also an important factor in crystal growth, defect generation, plasticity, etching, etc [93].

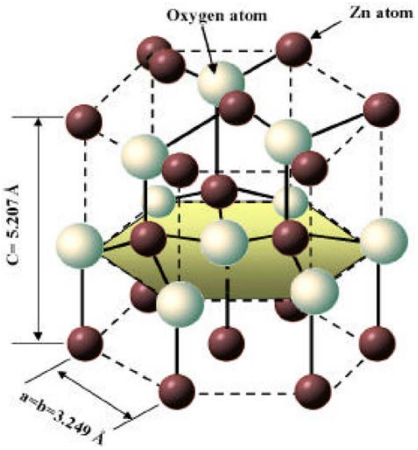

Figure 2.9 : The hexagonal wurtzite structure model of ZnO. The tetrahedral coordination of Zn-O is shown. O atoms are shown as larger white spheres while the Zn atoms are smaller brown spheres [93]

Table 2.1 : Physical properties of ZnO [79]

Properties	ZnO
Lattice parameters at 300 K	
$-a_o$ (nm)	0.3249
$-c_o$ (nm)	0.52069
$-c_o/a_o$	1.602(1.633*)
Density(g/cm^3)	5.606
Stable phase at 300 K	Wurtzite
Melting point (^{o}C)	1975
Thermal conductivity (Wcm^{-1} ^{o}C^{-1})	0.6, 1-1.2
Linear expansion coefficient (^{o}C)	a_o: 6.5 cm^3 x 10^{-6} c_o: 3.0 cm^3 x 10^{-6}
Static dielectric constant	8.656
Refractive index	2.008
Band gap (RT)	3.370 eV
Band gap (4 K)	3.437 eV
Exciton binding energy (meV)	60
Electron effective mass	0.24
Electron Hall mobility at 300 K (cm^2/Vs)	200
Hole effective mass	0.59
Hole Hall mobility at 300 K (cm^2/Vs)	5-50

*Value for an ideal hexagonal structures.

2.2.4 Synthesis of ZnO nanoparticles

Due to its broad application areas of ZnO, various synthetic routes have been employed to grow a variety of ZnO nanostructures, including nanoparticles,

nanowires, nanorods, nanotubes, nanobelts, and other complex morphologies [113, 114].

Zinc oxide particles -both nano and micrometric- can be produced by many different methods. These can be classified into metallurgical and chemical methods. The zinc oxide occurs in a very rich diversity of structures and offers a wide range of properties at the end of its synthesis. The variety of methods for ZnO production, such as vapour deposition, precipitation in water solution, hydrothermal synthesis, the sol-gel process, precipitation from microemulsions and mechanochemical processes, makes it possible to obtain products with particles differing in shape, size and spatial structure. [78] These methods are summarized at the Table 2.2.

Table 2.2 : Synthesis methods of ZnO Nanoparticles [78]

Method	Precursors	Synthesis conditions	Properties and applications
Mechano chemical process	$ZnCl_2$, Na_2CO_3, NaCl	calcination: 2 h, 600 °C	hexagonal structure; particles diameter: 21–25 nm
		400–800 °C	hexagonal structure; particles diameter: 18–35 nm
		400 °C	regular shape of particles; diameter ~27 nm, *BET*: 47 m^2/g
		0.5 h	particles diameter: 27–56 nm
		300–450 °C	particles diameter: ~51 nm, *BET*: 23 m^2/g
Precipitation process	$Zn(CH_3COO)_2$, and KOH as a water solutions	temperature of process: 20–80 °C; drying: 120 °C	particles diameter: 160–500 nm, *BET*: 4–16 m^2/g
	$Zn(CH_3COO)_2$, $(NH4)_2CO_3$, PEG10000 as a water solutions	drying: 12 h, 100 °C; calcination: 3 h, 450 °C	zincite structure; spherical particles (*D* ~ 30 nm); application: as a photocatlyst in photocatalytic degradation
	$Zn(NO_3)_2$	calcination: 2 h, 600 °C; aging: 240 h, 320 °C	wurtize structure; particles diameter: 50 nm; application: as a gas sensor
	$Zn(NO_3)_2$, NaOH	synthesis: 2 h; drying: 2 h, 100 °C	particles of spherical size of around 40 nm
	$ZnSO_4$, NH_4HCO_3, ethanol	drying: overnight, 100 °C; calcination: 300–500 °C	wurtize structure; crystallite size 9–20 nm; particle size *D*: ~12 nm, *BET*: 30–74 m^2/g
	$Zn(CH_3COO)_2$, NH_3 aq.	precipitation temperature: 85 °C; drying: 10 h, 60 °C	hexagonal structure, shape of rods, flower-like particles: *L*: 150 nm, *D*: 200 nm
	$ZnSO_4$, NH_4OH, NH_4HCO_3	reaction: 30 min, 60 °C; drying: 12 h, 100 °C; calcination: 2 h, 400 °C	hexagonal structure, flake-like morphology (*D*: 0.1–1 μm, *L*: 60 nm)

	microsized ZnO powder, NH_4HCO_3	reaction: ~2 h, 25 °C; drying: 80 °C; calcination:1 h, 350 °C	hexagonal wurtize structure; flower-like and rod-like shape (*D*: 15–25 nm, *BET*: 50–70 m^2/g)
	$Zn(CH_3COO)_2$, NaOH	reaction: 30 min, 75 °C; drying: overnight, room temperature	hexagonal structure; flower shape (*L*: >800 nm); application: antimicrobial activity
Precipitation in the presence of surfactants	$ZnCl_2$, NH_4OH, CTAB	aging: 96 h, ambient temperature, calcination: 2 h, 500 °C	incite structure; particles diameter: 54–60 nm, *BET* = ~17 m^2/g
	$Zn(NO_3)_2$, NaOH, SDS, TEA (triethanolamine)	precipitation: 50–55 min, 101 °C	wurtize structure, shape of rod-like (*L*: 3.6 μm, *D*: 400–500 nm) shape of nut-like and rice-like, size: 1.2–1.5 μm zincite structure; aggregate
Sol-gel	$Zn(CH_3COO)_2$, oxalic acid, ethanol and methanol	reaction temperature: 60 °C; drying: 24 h, 80 °C; calcination: 500 °C	particles: ~100 nm; shape of rod; particles *L*: ~500 nm, *D*: ~100 nm; *BET*: 53 m/g; application: decontamination of sarin (neuro-toxic agent)
	$Zn(CH_3COO)_2$, oxalic acid ($C_2H_2O_4$), ethanol	reaction: 50 °C, 60 min; dried of gel: 80 °C, 20 h; calcined: under flowing air for 4 h at 650 °C	hexagonal wurtize structure; uniform, spherically shaped of particles
	$Zn(CH_3COO)_2$, diethanolamine, ethanol	reaction: room temperature; annealed of sol: 2 h, 500 °C	hexagonal wurtize structure; particles: nanotubes of 70 nm
Solvothermal hydrothermal and microwave techniques	$ZnCl_2$, NaOH	reaction: 5–10 h, 100–220 °C in teflon-lined autoclave	particles morphology: bullet-like (100–200 nm), rod-like (100–200 nm), sheet (50–200 nm), polyhedron (200–400 nm), crushed stone-like (50–200 nm)
	$Zn(CH_3COO)_2$, NaOH, HMTA (hexamethylenetetraamine)	reaction: 5–10 h, 100–200 °C; HMTA concentration: 0–200 ppm	spherical shape; particles diameter: 55–110 nm
	$Zn(CH_3COO)_2$, $Zn(NO_3)_2$, LiOH, KOH, NH_4OH	reaction: 10–48 h, 120–250 °C	hexagonal (wurtize) structure, size of microcrystallites: 100 nm–20 μm
	$Zn(CH_3COO)_2$, NH_3, zinc 2-ethylhexanoate, TMAH, ethanol, 2-propanol	time of autoclaving: 15 min, 2–72 h; final pH: 7–10	particles with irregular ends and holes; aggregates consist particles of 20–60 nm, *BET*: 0.49–6.02 m^2/g
	trimethylamine N-oxide, 4-picoline N-oxide, HCl, toluene, ethylenediamine	reaction: 24–100 h, 180 °C	wurtize structure; particles morphology: nanorods (40–185 nm), nanoparticles (24–60 nm)

	(EDA), N,N,N',N'-tetramethylethylenediamine (TMEDA)		
	$Zn(CH_3COO)_2$, $Zn(NO_3)_2$, ethanol, imidazolium	reaction: 150–180 °C; drying: 80 °C in vacuum oven;	hexagonal (wurtize) structure, hollow microspheres (2–5 μm) consisted nano-sized particles and contained channels (10 nm);
	tetrafluoroborate ionic liquid	calcinations: 500 °C	hollow microspheres consisted of nanorods (~20 nm); flower-like microspheres (2.5 μm)
	zinc acetylacetonate, methoxy-ethoxy- and n-butoxyethanol, zinc oximate	precursor concentration: 2.5–10 wt%; microwave heating: 800 W, 4 min; drying: 75 °C in air	zincite structure; average crystallite size: 9–31 nm; particles diameter: 40–200 nm; *BET*: 10–70 m^2/g
	$Zn(NO_3)_2$, deionized water, HMT (hexamethylenetetramine)	microwave heating: 2 min, 90 °C; drying: 2 h, 60 °C	hexagonal wurtize structure, nanorod and nanowire shape (*L*: ~0.7 μm, *D*: ~280 nm); application: electronic and optoelectronic devices
Emulsion	$Zn(NO_3)_2$, surfactant (ABS, Tween-80 and 40, $C_{21}H_{38}BrN$)	reaction: 25 °C, pH~8; drying: 24 h, 80 °C; calcination: 2 h, 600 °C	grain size: cationic surfactants (40–50 nm), nonionic surfactants (20–50 nm), anionic surfactants (~20 nm) particles morphology: irregular particles aggregates (2–10 μm); needle-shaped (*L*: 200–600 nm, T: 90–150 nm);
	$Zn(C_{17}H_{33}COO)_2$, NaOH, decane, water, ethanol	reaction: 2 h, room temperature or 90 °C	nearly spherical and hexagonal (*D*: 100–230 nm); spherical and pseudospherical aggregates (*D*: 150 nm)
	$Zn(CH_3COO)_2$, heptanes, Span-80, NH_4OH	reaction: 1 h; aging: 2.5 h; drying: in rotary evaporator; calcination: 2 h, 700–1000 °C	hexagonal structure; spherical shape; particles diameter: 0.05–0.15 μm
	$Zn(CH_3COO)_2$, NaOH and KOH, cyclohexane, non-ionic surfactants	reaction: ambient temperature; drying: 24 h, 120 °C	hexagonal structure; particles morphology: solids (164–955 nm, *BET*: 8 m^2/g), ellipsoids (459–2670 nm, *BET*: 10.6 m_2/g), rods (396–825 nm, *BET*: 12 m^2/g), flakes (220–712 nm, *BET*: 20 m^2/g); crystallites size: 32–77 nm; application: as a photocatalyst
Micro emulsion	$Zn(NO_3)_2$, NaOH, heptane, hexanol, Triton X-100, PEG400	reaction: 15 h, 140 °C; drying: 60 °C	hexagonal (wurtize) structure; particles morphology: needle (*L*: 150–200 nm, *D*: ~55 nm), nanocolumns (*L*: 80–100 nm,

			D: 50-80 nm), spherical (~45 nm)
	$Zn(NO_3)_2$, oxalic acid, isooctane, benzene, ethanol, diethyl ether, chloroform, acetone, methanol, Aerosol OT	reaction: 24 h, 60–70 °C; drying: 1 h, 100 °C; calcination: 3 h, 300–500 °C	hexagonal wurtize structure, spherical shape (15–24 nm), rods shape (*L*: 66–72 nm, *D*: 21–28 nm)
	$ZnCl_2$,$Zn(CH_3COO)_2$, heptane, BTME (1,2-trimethoxysilyl)ethane, TMOS (tetramethoxysilane), methanol, Aerosol OT, NaOH	reaction: 2–3 h, room temperature or 40 °C; drying: under vacuum overnight; calcinations: 24 h, 700 °C	hexagonal structure, uniformly dispersed small particles, size of particles ~10 nm
Other method	$Zn(NO_3)_2$, deionized water, HMT (hexamethylenetetramine)	ultrasonic irradiation: 30 min, 80 °C; drying: 2 h, 60 °C	hexagonal wurtize structure, nanorod and nanowire shape (*L*: ~1 μm, *D*: ~160 nm); application: electronic and optoelectronic devices
	micron scale zinc metal powder	feed rate: 1 g/min; plasma power: 1 kW; O_2 flow rate: 2.5 lpm; N_2 flow rate: 12.5 lpm; reaction: 900 °C	nanowires shape (*L*: 1–30 μm, *D*: 5–50 nm) application: as hydrodesulfurization catalyst
	diethylzinc (DEZ), oxygen	helium as a carrier gas	wurtize structure; average particle size: 9 nm

**BET*—surface area calculated based on BET equation; *D*—particles diameter; *L*—particles length.

2.2.5 Applications of zinc oxide

Because of its various and useful properties, both chemical and physical, zinc oxide is widely utilized in many areas. It plays a significant role in a very wide range of applications, ranging from tyres to ceramics, from pharmaceuticals to agriculture, and from paints to chemicals. [78]

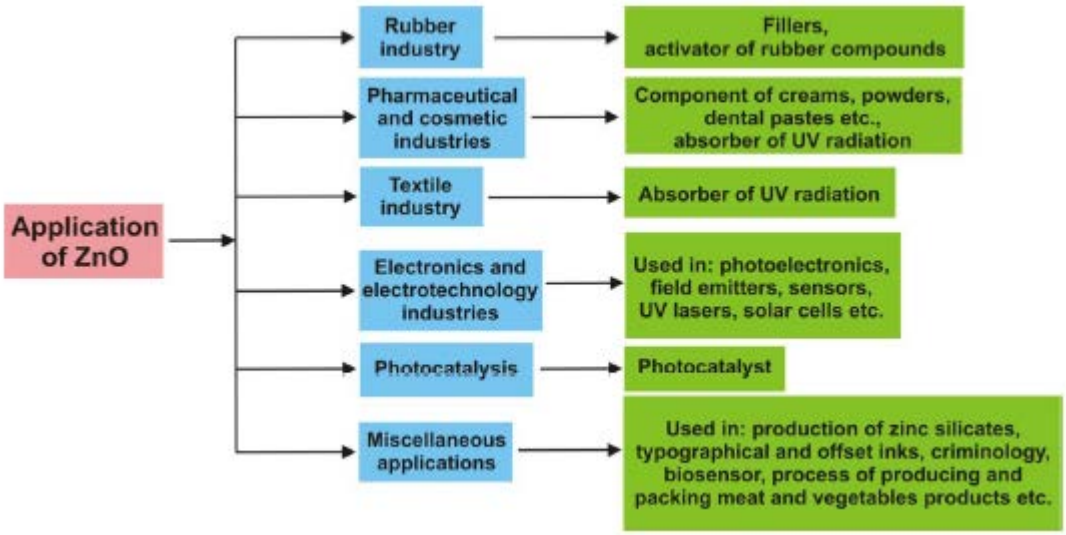

Figure 2.10 : Shematic representation of applications of ZnO [78]

3. EXPERIMENTAL PART

3.1 Materials

Zinc (II) nitrate hexahydrate ($Zn^{II}(NO_3)_2.6H_2O$, 98%; Sigma-Aldrich), zinc chloride ($ZnCl_2$, ≥98%, Sigma-Aldrich), ammonium hydroxide solution (NH_4OH, 28.0-30.0% NH_3 basis, Sigma-Aldrih). Benzyl bromide (98%, Sigma-Aldrich), phenylacetylene (98%, Sigma-Aldrich), ethyl 2-bromopropionate (99%, Sigma-Aldrich), 1-bromooctane (98%, Fluka), aniline (99.5%, Aldrich), 2-nitrobenzyl chloride (99%, Sigma-Aldrich), 1,7-dibromoheptane (97%, Sigma-Aldrich), (1-bromoethyl)benzene (97%, Sigma-Aldrich), 3-ethynylthiophene (96%, Sigma-Aldrich), propargyl acrylate (98%, Sigma-Aldrich), propargyl alcohol (99%, Sigma-Aldrich), 1,4-diethynylbenzene (96%, Sigma-Aldrich), sodium azide (NaN_3, 99%, Panreac), and copper(II) chloride ($Cu^{II}Cl_2$, 99%, Acros Organics) were used as received without any further purification. Sodium nitrite ($NaNO_2$, Carlo Erba), magnesium sulfate ($MgSO_4$, Alfa Aesar, 99.5%), sodium bicarbonate ($NaHCO_3$, ≥99.7%, Sigma-Aldrich) were used as received.

N,N,N′,N″,N″-pentamethyldiethylenetriamine (PMDETA, 99%, Sigma-Aldrich*)* was purified by passing through basic alumina (Al_2O_3) prior to use. Dimethyl sulfoxide (DMSO), diethyl ether ($(C_4H_5)_2O$), acetonitrile (CH_3CN) were purchased from Merck and used as received.

3.2 Instrumentation

Light Source

A Ker-Vis blue photoreactor equipped with 6 lamps (Philips TL-D 18 W) emitting light nominally at 400–500 nm was used in all click experiments. The light intensity was 45 $mW.cm^{-2}$ as measured by Delta Ohm model HD-9021 radiometer.

UV-vis spectrometer

UV-visible spectra were recorded with a Shimadzu UV-1601 spectrometer.

^{1}H-Nuclear magnetic resonance spectroscopy

^{1}H-NMR spectra were recorded in deuterated chloroform ($CDCl_3$) with $Si(CH_3)_4$ as an internal standard at 500 MHz on a Agilent VNMRS 500 spectrometer at room temperature.

Fourier transform infrared spectroscopy

Fourier transform infrared (FTIR) spectra were recorded on Perkin−Elmer FTIR Spectrum One spectrometer with an ATR Accessory (ZnSe, PikeMiracle Accessory) and cadmium telluride (MCT) detector.

Gel permeation chromatography

Gel permeation chromatography (GPC) measurements were performed on a Viscotek GPC max auto sampler system consisting of a pump, a Viscotek UV detector, and Viscotek a differential refractive index (RI) detector with three ViscoGEL GPC columns (G2000H HR, G3000H HR, and G4000H HR, 7.8 mm internal diameter, 300 mm length) in series. The effective molecular weight ranges were 456 − 42800, 1050 − 107000, and 10200 − 2890000, respectively. THF was used as an eluent at flow rate of 1.0 mL min^{-1} at 30 °C. Both detectors were calibrated with PS standards having narrow-molecular-weight distribution. Data were analyzed using ViscotekOmniSEC Omni-01 software.

Scanning electron microscope (SEM)

Electron microscopic images were taken on a JEOL Scanning Electron Microscope (JSM-7600F, Japan).

X-ray diffraction patterns (XRD)

X-ray diffraction patterns (XRD) were obtained with a computer controlled X'Pert Explorer, PAN analytical diffractometer.

3.3 Preparation of Zinc Oxide Nanoparticles (ZnO NPs)

ZnO NPs were synthesized by a hydrothermal method using the aqueous mixtures of $ZnCl_2$ and NH_4OH as source materials.[115] In a typical run, a solution of NH_4OH was added drop wise into 0.1 M $ZnCl_2$ solution made in 100 mL of deionized water under vigorous stirring. Upon reaching the pH of the solution to 10.2, the addition of NH_4OH was stopped and the reaction was stirred for more 1 h. The resultant was then transferred into a Teflon-lined autoclave and heated up to 150 ^oC for 3 h. After terminating the reaction, the autoclave was allowed to cool at room temperature and finally white precipitates were obtained which were washed with methanol several times and dried at room temperature. The dried products were then calcined at 400 ^oC for 3 h and characterized in detail in terms of their structural, optical, photocatalytic and sensing properties.

3.4 Procedures for the Preparation of Azide Components

General procedure A:[116]

To a solution of the corresponding bromide (or chloride) compound (15 mmol, 1.0 eq) in 200 mL of dimethyl sulfoxide was added NaN_3 in excess (1.5 eq). The solution was stirred for at least 2 h at room temperature. Afterwards water (200 mL) was added and the mixture was allowed to cool down to room temperature. The aqueous solution was extracted with diethyl ether (3 × 100 mL). The organic layers were merged and washed with water (2 × 100 mL) and brine (100 mL). After drying over $MgSO_4$, the ether was evaporated under reduced pressure to give corresponding azides.

Procedure B:[117]

Aniline (15 mmol, 1 eq.) was added to 80 mL of hydrochloric acid (17%) at room temperature followed by drop wise addition of ethanol to obtain a clear solution. The solution was cooled to 0 °C and $NaNO_2$ (1.5 eq.) was added in small portions. After stirring at 0 °C for 30 minutes, NaN3 (1.5 eq.) was slowly added and the mixture was stirred for further 2 h at room temperature. The reaction mixture was extracted with diethyl ether (3 × 100 mL) and the combined organic fractions were washed with saturated $NaHCO_3$ solution (3 × 50 mL) and with brine (50 mL). After drying over $MgSO_4$, the ether was removed under reduced pressure to obtain phenyl azide.

3.5 General Procedure for the Preparation of 1,4-Disubstituted Triazoles

In a Pyrex tube $Cu^{II}Cl_2$ (6.75 mg, 0.05 mmol) and PMDETA (10.5 µL, 0.10 mmol) were dissolved in 3 mL of MeCN. To the mixture were added 1 mmol azide, 1 mmol alkyne, and 20 mg of ZnO NPs. The mixture was then irradiated in using a Ker-Vis photoreactor equipped with six lamps emitting light at 400-500 nm with the light intensity of 45 mW cm^{-2} at room temperature. After irradiation, nanoparticles were filtered off and the resultant was purified by a short column chromatography.

4. RESULTS AND DISCUSSION

Herein, a visible light-induced CuAAC strategy was carried out benefiting from the electron transfer reactions of ZnO NPs to achieve the required catalyst for CuAAC. ZnO NPs used in this study were prepared via a simple hydrothermal process according to a previously reported procedure[115] yielding well-crystalline NPs in large quantity. Figure 4.1 shows FESEM image of the obtained nanoparticles in the spherical form with an average diameter of 50 nm. The XRD pattern is shown in Figure 4.2 that indicates characteristic peaks of the synthesized ZnO NPs.

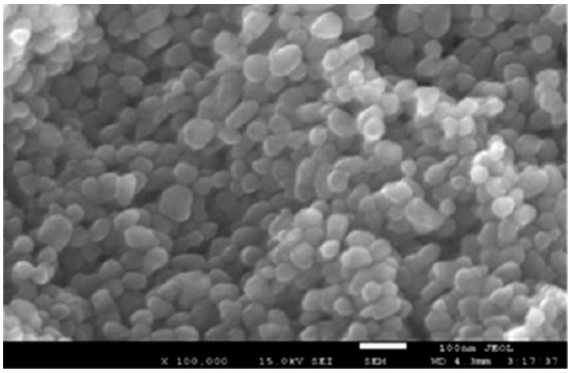

Figure 4.1 : FESEM image of ZnO NPs (scale bar 100 nm)

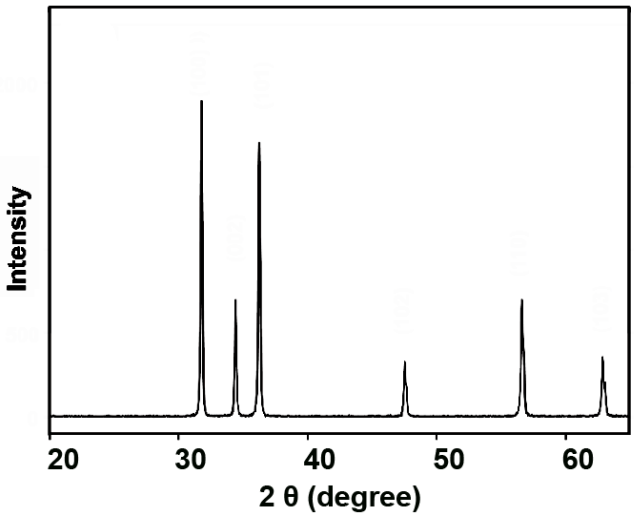

Figure 4.2 : XRD patterns of ZnO NPs

Figure 4.3 shows the UV-vis spectra of the NPs strong absorption between 400-500 nm at UV and visible regions. In order to evaluate the potential of these nanoparticles as the photocatalyst for reducing Cu(II) to Cu(I), UV-vis studies were conducted.

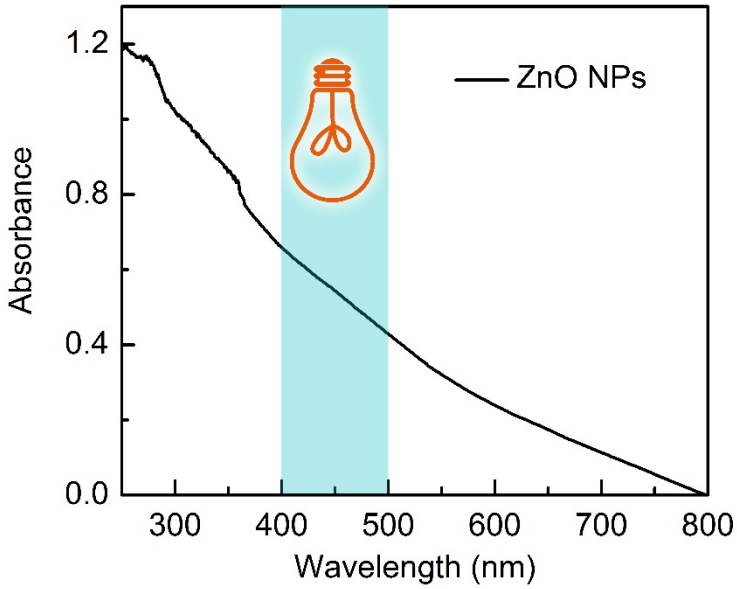

Figure 4.3 : UV-vis spectra of ZnO NPs.

A solution of copper(II) chloride/N,N,N′,N′,N″-pentamethyldiethylenetriamine ($CuIICl_2$/PMDETA) in acetonitrile in the presence of ZnO NPs exposed to visible light showed a decrease in the intensity of the absorption band of Cu(II) in the 500 to 1000 nm region (Figure 4.4). This was attributed to the transformation from the Cu(II) d^9 configuration to the Cu(I) d^{10} configuration indicative of successful reduction of Cu(II) by the photogenerated electrons stemming from the nanoparticles.

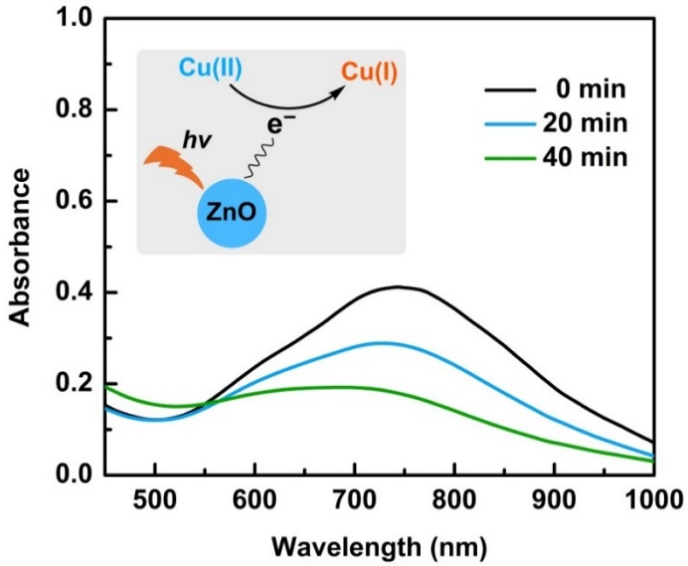

Figure 4.4 : Photoinduced reduction of Cu(II) species with the help of zinc oxide nanoparticles as evidenced by UV-vis measurements: disappearance of the characteristic band of Cu(II) in a solution of $Cu(II)Cl_2$/PMDETA in acetonitrile in the presence of the nanoparticles irradiated under visible light clearly indicates the reduction of Cu(II) (inset: schematic representation of the photoinduced reduction of Cu(II) to Cu(I) by photogenerated electrons from zinc oxide nanoparticles, $[Cu(II)Cl_2] = 1.5 \times 10^{-3}$ M).

Having shown the efficient photoreduction of Cu(II) by ZnO NPs, these nanoparticle were used to photochemically induce the CuAAC process. A model reaction was designed employing benzyl azide and phenylacetylene as the model substitutes in the presence of $Cu^{II}Cl_2$/PMDETA as the catalyst in acetonitrile to investigate the kinetics of the photoinduced CuAAC using ZnO NPs under light (Figure 4.5-a). The kinetics of the reaction were followed by FTIR spectroscopy as the azide peak around 2100 cm^{-1} gradually disappeared as the reaction proceeded and therefore conversions were obtained by integrating the peak area of the azide functionality between 2000 and 2200 cm^{-1}. Irradiating under UV light (350 nm), the reaction completed after 40 min whereas using a visible light source (400-500 nm) took 60 min to have the reaction completed (Figure 4.5-b). ^1H NMR spectra of the isolated product shown in Figure 4.5-c clearly confirm the successful clicking of benzyl azide and phenylacetylene and all characteristics of the clicked product. Control experiments either in the absence of nanoparticles or in the dark, giving only traces of the final product, revealed the necessity of the initiating components for the reaction to occur. We chose to proceed with the visible light in the succeeding parts.

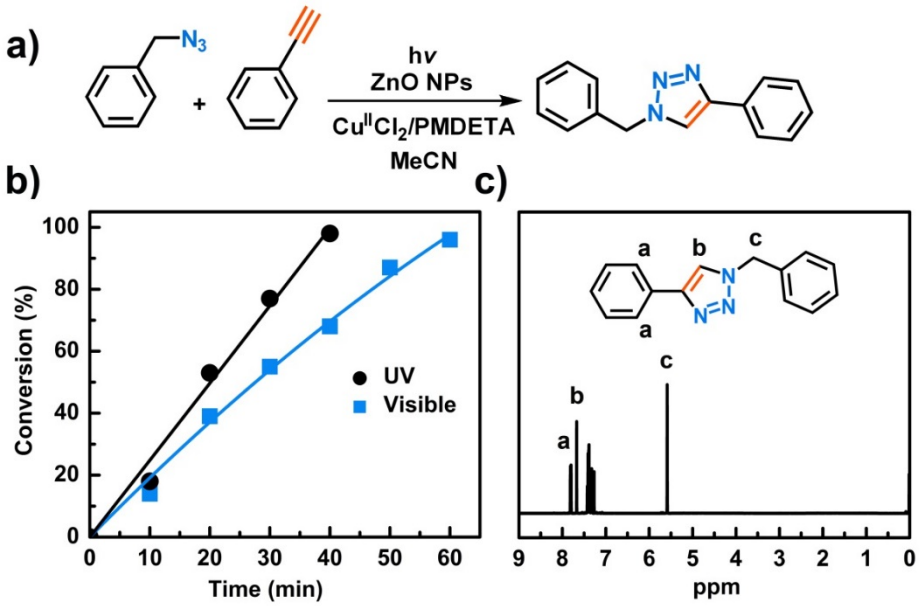

Figure 4.5 : Kinetics of the photoinduced CuAAC using zinc oxide nanoparticles: a) schematic representation of the model reaction of benzyl azide and phenylacetylene, b) conversion versus irradiation time for the model reaction illuminating under UV and visible light, and c) ^{1}H NMR spectra of the final isolated product of the model reaction showing characteristic peaks of the clicked product.

The scope of the system was examined for a variety of azide and alkyne components (Figure 4.6). Many functional groups were compatible with the system including thiophene, propargyl moieties, ester, nitro, aliphatic, and aromatic substrates with good yields at ambient conditions and under visible light irradiation.

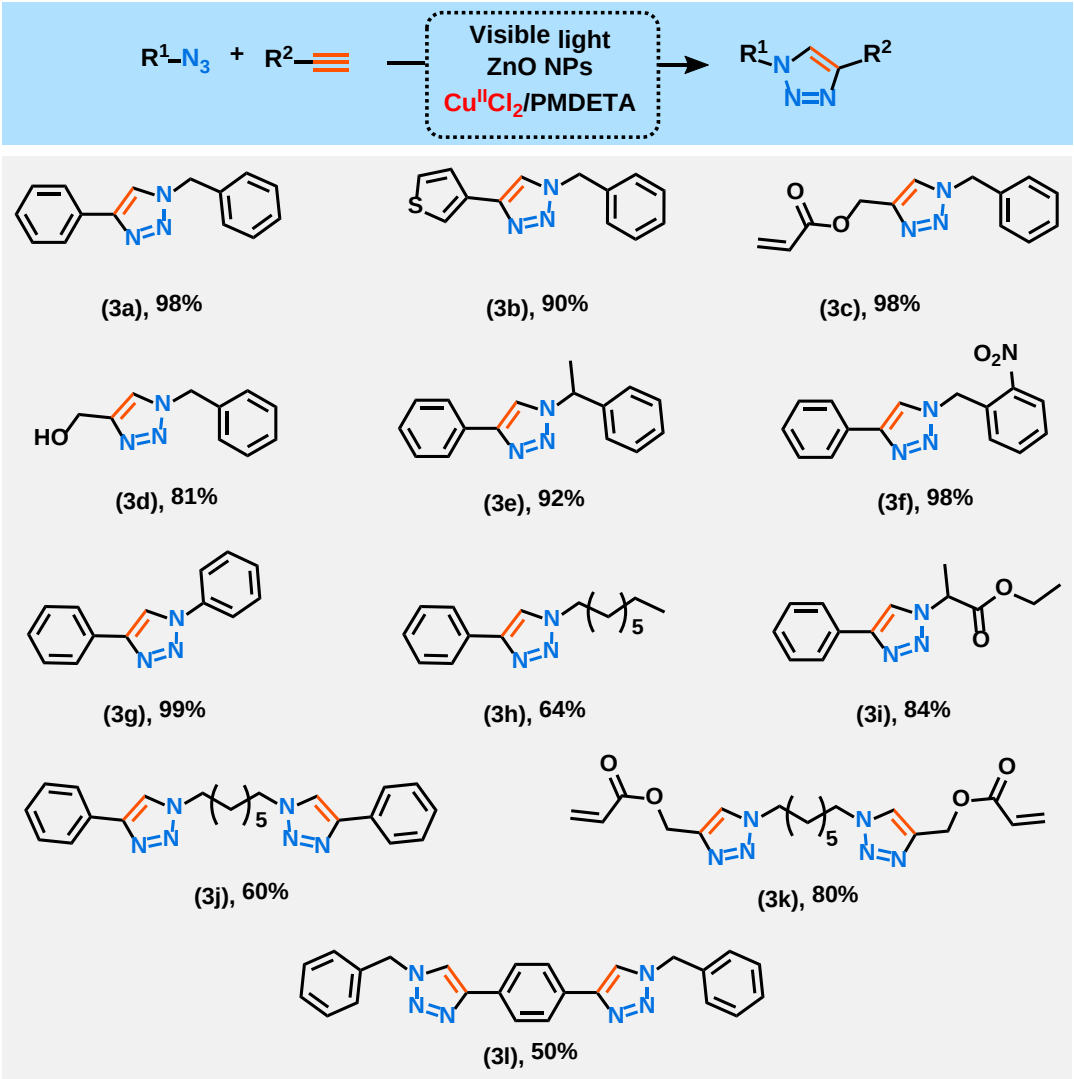

Figure 4.6 : Visible light-induced CuAAC of several of azides and alkynes using zinc oxide nanoparticles as photocatalyst.

When using propargyl moieties as the alkyne component, propargyl acrylate reached to 98% yield (3c) after 2 h irradiation under visible light while propargyl alcohol was rather slow and gave 81% yield (3d). Aliphatic azides were efficiently tried (3h and 3i). Bifunctional azide and alkyne were also tested. Notably clicking a biazide, 1,7-diazidoheptane, with phenylacetylene resulted in a white solid with 60% of yield which was insoluble in common organic solvents (3j). However, it resulted in a soluble adduct when propargyl acrylate was used instead of phenylacetylene giving a yield of 80% (3k). 1,4-Diethynylbenzene bearing two alkyne functionalities clicked with benzyl azide was also quite insoluble in the media and reached to 58% yield (3l). This insolubility would be probably due to the higher number of triazole and aromatic rings present in 3j and 3l, making them more rigid.

5. CONCLUSION

In conclusion, the photocatalytic activity of semiconductor nanoparticles has demonstrated in photoinduced CuAAC click reactions. The reduction of Cu(II) was smoothly achieved by ZnO NPs upon visible light irradiation, and various azides and alkynes were successfully clicked together. Several studies dealing with expanding the scope of the photoinduced click reactions, especially copper(I)-catalyzed processes, are currently underway. These works will design novel copper-based photocatalysts with the aim of achieving better mechanistic understanding of such systems and gaining spatiotemporal control over the photoinduced CuAAC process for (macro)molecular tailoring.

REFERENCES

[1] **Cahen, D. and Lubomirsky, I.** (2008). Energy, the global challenge, and materials, *Materials Today*, 11, 16-20.

[2] **Adams, D.M., Brus, L., Chidsey, C.E.D., Creager, S., Creutz, C., Kagan, C.R., Kamat, P.V., Lieberman, M., Lindsay, S., Marcus, R.A., Metzger, R.M., Michel-Beyerle, M.E., Miller, J.R., Newton, M.D., Rolison, D.R., Sankey, O., Schanze, K.S., Yardley, J., and Zhu, X.Y.** (2003). Charge transfer on the nanoscale: Current status, *Journal of Physical Chemistry B*, 107, 6668-6697.

[3] **Kisch, H.** (2013). Semiconductor photocatalysismechanistic and synthetic aspects, *Angewandte Chemie International Edition*, 52, 812-847.

[4] **Kolb, H.C., Finn, M.G., and Sharpless, K.B.** (2001). Click chemistry: Diverse chemical function from a few good reactions, *Angewandte Chemie International Edition*, 40, 2004-2021.

[5] **Rostovtsev, V.V., Green, L.G., Fokin, V.V., and Sharpless, K.B.** (2002). A stepwise huisgen cycloaddition process: Copper(i)-catalyzed regioselective "ligation" of azides and terminal alkynes, *Angewandte Chemie International Edition*, 41, 2596-2599.

[6] **Tornoe, C.W., Christensen, C., and Meldal, M.** (2002). Peptidotriazoles on solid phase: 1,2,3 -triazoles by regiospecific copper(i)-catalyzed 1,3-dipolar cycloadditions of terminal alkynes to azides, *Journal of Organic Chemistry*, 67, 3057-3064.

[7] **Moses, J.E. and Moorhouse, A.D.** (2007). The growing applications of click chemistry, *Chemical Society Reviews*, 36, 1249-1262.

[8] **Xi, W.X., Scott, T.F., Kloxin, C.J., and Bowman, C.N.** (2014). Click chemistry in materials science, *Advanced Functional Materials*, 24, 2572-2590.

[9] **Lutz, J.-F.** (2007). 1,3-dipolar cycloadditions of azides and alkynes: A universal ligation tool in polymer and materials science, *Angewandte Chemie International Edition*, 46, 1018-1025.

[10] **Lutz, J.-F. and Borner, H.G.** (2008). Modern trends in polymer bioconjugates design, *Progress in Polymer Science*, 33, 1-39.

[11] **Kolb, H.C. and Sharpless, K.B.** (2003). The growing impact of click chemistry on drug discovery, *Drug Discovery Today*, 8, 1128-1137.

[12] **Worrell, B.T., Malik, J.A., and Fokin, V.V.** (2013). Direct evidence of a dinuclear copper intermediate in cu(i)-catalyzed azide-alkyne cycloadditions, *Science*, 340, 457-460.

[13] **Tasdelen, M.A. and Yagci, Y.** (2013). Light-induced click reactions, *Angewandte Chemie International Edition*, 52, 5930-5938.

[14] **Tasdelen, M.A. and Yagci, Y.** (2010). Light-induced copper(i)-catalyzed click chemistry, *Tetrahedron Letters*, 51, 6945-6947.

[15] **Sandmann, B., Happ, B., Vitz, J., Hager, M.D., Burtscher, P., Moszner, N., and Schubert, U.S.** (2013). Photoinduced polyaddition of multifunctional azides and alkynes, *Polymer Chemistry*, 4, 3938-3942.

[16] **Ritter, S.C. and Koenig, B.** (2006). Signal amplification and transduction by photo-activated catalysis, *Chemical Communications*, 4694-4696.
[17] **Adzima, B.J., Tao, Y.H., Kloxin, C.J., DeForest, C.A., Anseth, K.S., and Bowman, C.N.** (2011). Spatial and temporal control of the alkyne-azide cycloaddition by photoinitiated cu(ii) reduction, *Nature Chemistry*, 3, 256-259.
[18] **Tasdelen, M.A., Yilmaz, G., Iskin, B., and Yagci, Y.** (2012). Photoinduced free radical promoted copper(i)-catalyzed click chemistry for macromolecular syntheses, *Macromolecules*, 45, 56-61.
[19] **Alzahrani, A.A., Erbse, A.H., and Bowman, C.N.** (2014). Evaluation and development of novel photoinitiator complexes for photoinitiating the copper-catalyzed azide-alkyne cycloaddition reaction, *Polymer Chemistry*, 5, 1874-1882.
[20] **Yagci, Y., Tasdelen, M.A., and Jockusch, S.** (2014). Reduction of cu(ii) by photochemically generated phosphonyl radicals to generate cu(i) as catalyst for atom transfer radical polymerization and azide-alkyne cycloaddition click reactions, *Polymer*, 55, 3468-3474.
[21] **Doran, S., Murtezi, E., Barlas, F.B., Timur, S., and Yagci, Y.** (2014). One-pot photo-induced sequential cuaac and thiol-ene click strategy for bioactive macromolecular synthesis, *Macromolecules*, 47, 3608-3613.
[22] **Yilmaz, G., Iskin, B., and Yagci, Y.** (2014). Photoinduced copper(i)-catalyzed click chemistry by the electron transfer process using polynuclear aromatic compounds, *Macromolecular Chemistry and Physics*, 215, 662-668.
[23] **Kolb, H.C., Finn, M.G., and Sharpless, K.B.** (2001). Click chemistry: Diverse chemical function from a few good reactions, *Angewandte Chemie-International Edition*, 40, 2004-+.
[24] **Liang, L. and Astruc, D.** (2011). The copper(i)-catalyzed alkyne-azide cycloaddition (cuaac) "click" reaction and its applications. An overview, *Coordination Chemistry Reviews*, 255, 2933-2945.
[25] **Yuan, Y. and Liang, G.** (2014). A biocompatible, highly efficient click reaction and its applications, *Organic & Biomolecular Chemistry*, 12, 865-871.
[26] **Rostovtsev, V.V., Green, L.G., Fokin, V.V., and Sharpless, K.B.** (2002). A stepwise huisgen cycloaddition process: Copper(i)-catalyzed regioselective "ligation" of azides and terminal alkynes, *Angewandte Chemie-International Edition*, 41, 2596-2599.
[27] **Tornoe, C.W., Christensen, C., and Meldal, M.** (2002). Peptidotriazoles on solid phase: [1,2,3]-triazoles by regiospecific copper(i)-catalyzed 1,3-dipolar cycloadditions of terminal alkynes to azides, *Journal of Organic Chemistry*, 67, 3057-3064.
[28] **Franc, G. and Kakkar, A.K.** (2009). Diels-alder "click" chemistry in designing dendritic macromolecules, *Chemistry-a European Journal*, 15, 5630-5639.
[29] **Tasdelen, M.A.** (2011). Diels-alder "click" reactions: Recent applications in polymer and material science, *Polymer Chemistry*, 2, 2133-2145.
[30] **Hizal, G., Tunca, U., and Sanyal, A.** (2011). Discrete macromolecular constructs via the diels-alder "click" reaction, *Journal of Polymer Science Part a-Polymer Chemistry*, 49, 4103-4120.
[31] **Sanyal, A.** (2010). Diels-alder cycloaddition-cycloreversion: A powerful combo in materials design, *Macromolecular Chemistry and Physics*, 211, 1417-1425.

[32] **Kumaraswamy, G., Ankamma, K., and Pitchaiah, A.** (2007). Tandem epoxide or aziridine ring opening by azide/copper catalyzed [3+2] cycloaddition: Efficient synthesis of 1,2,3-triazolo beta-hydroxy or beta-tosylamino functionality motif, *Journal of Organic Chemistry*, 72, 9822-9825.

[33] **Heredia, K.L., Tolstyka, Z.P., and Maynard, H.D.** (2007). Aminooxy end-functionalized polymers synthesized by atrp for chemoselective conjugation to proteins, *Macromolecules*, 40, 4772-4779.

[34] **Dirksen, A. and Dawson, P.E.** (2008). Rapid oxime and hydrazone ligations with aromatic aldehydes for biomolecular labeling, *Bioconjugate Chemistry*, 19, 2543-2548.

[35] **Bahta, M., Liu, F., Kim, S.E., Stephen, A.G., Fisher, R.J., and Burke, T.R.** (2012). Oxime-based linker libraries as a general approach for the rapid generation and screening of multidentate inhibitors, *Nature Protocols*, 7, 686-702.

[36] **Campos, L.M., Killops, K.L., Sakai, R., Paulusse, J.M.J., Damiron, D., Drockenmuller, E., Messmore, B.W., and Hawker, C.J.** (2008). Development of thermal and photochemical strategies for thiol-ene click polymer functionalization, *Macromolecules*, 41, 7063-7070.

[37] **Killops, K.L., Campos, L.M., and Hawker, C.J.** (2008). Robust, efficient, and orthogonal synthesis of dendrimers via thiol-ene "click" chemistry, *Journal of the American Chemical Society*, 130, 5062-5064.

[38] **Hoyle, C.E. and Bowman, C.N.** (2010). Thiol-ene click chemistry, *Angewandte Chemie-International Edition*, 49, 1540-1573.

[39] **Hoyle, C.E., Lowe, A.B., and Bowman, C.N.** (2010). Thiol-click chemistry: A multifaceted toolbox for small molecule and polymer synthesis, *Chemical Society Reviews*, 39, 1355-1387.

[40] **Lowe, A.B., Hoyle, C.E., and Bowman, C.N.** (2010). Thiol-yne click chemistry: A powerful and versatile methodology for materials synthesis, *Journal of Materials Chemistry*, 20, 4745-4750.

[41] **Haldon, E., Carmen Nicasio, M., and Perez, P.J.** (2015). Copper-catalysed azide-alkyne cycloadditions (cuaac): An update, *Organic & Biomolecular Chemistry*, 13, 9528-9550.

[42] **Hein, J.E. and Fokin, V.V.** (2010). Copper-catalyzed azide-alkyne cycloaddition (cuaac) and beyond: New reactivity of copper(i) acetylides, *Chemical Society Reviews*, 39, 1302-1315.

[43] **Himo, F., Lovell, T., Hilgraf, R., Rostovtsev, V.V., Noodleman, L., Sharpless, K.B., and Fokin, V.V.** (2005). Copper(i)-catalyzed synthesis of azoles. Dft study predicts unprecedented reactivity and intermediates, *Journal of the American Chemical Society*, 127, 210-216.

[44] **Tron, G.C., Pirali, T., Billington, R.A., Canonico, P.L., Sorba, G., and Genazzani, A.A.** (2008). Click chemistry reactions in medicinal chemistry: Applications of the 1,3-dipolar cycloaddition between azides and alkynes, *Medicinal Research Reviews*, 28, 278-308.

[45] **Zhang, L., Chen, X.G., Xue, P., Sun, H.H.Y., Williams, I.D., Sharpless, K.B., Fokin, V.V., and Jia, G.C.** (2005). Ruthenium-catalyzed cycloaddition of alkynes and organic azides, *Journal of the American Chemical Society*, 127, 15998-15999.

[46] **Chowdhury, C., Mandal, S.B., and Achari, B.** (2005). Palladium-copper catalysed heteroannulation of acetylenic compounds: An expeditious

synthesis of isoindoline fused with triazoles, *Tetrahedron Letters*, 46, 8531-8534.

[47] **Golas, P.L., Tsarevsky, N.V., Sumerlin, B.S., and Matyjaszewski, K.** (2006). Catalyst performance in "click" coupling reactions of polymers prepared by atrp: Ligand and metal effects, *Macromolecules*, 39, 6451-6457.

[48] **Partyka, D.V., Updegraff, J.B., III, Zeller, M., Hunter, A.D., and Gray, T.G.** (2007). Carbon-gold bond formation through 3+2 cycloaddition reactions of gold(i) azides and terminal alkynes, *Organometallics*, 26, 183-186.

[49] **Stowell, M.H.B., McPhillips, T.M., Rees, D.C., Soltis, S.M., Abresch, E., and Feher, G.** (1997). Light-induced structural changes in photosynthetic reaction center: Implications for mechanism of electron-proton transfer, *Science*, 276, 812-816.

[50] **Hong, V., Udit, A.K., Evans, R.A., and Finn, M.G.** (2008). Electrochemically protected copper(i)-catalyzed azide-alkyne cycloaddition, *ChemBioChem*, 9, 1481-1486.

[51] **Adzima, B.J., Tao, Y., Kloxin, C.J., DeForest, C.A., Anseth, K.S., and Bowman, C.N.** (2011). Spatial and temporal control of the alkyne-azide cycloaddition by photoinitiated cu(ii) reduction, *Nature Chemistry*, 3, 256-259.

[52] **Chen, R.T., Marchesan, S., Evans, R.A., Styan, K.E., Such, G.K., Postma, A., McLean, K.M., Muir, B.W., and Caruso, F.** (2012). Photoinitiated alkyne-azide click and radical cross-linking reactions for the patterning of peg hydrogels, *Biomacromolecules*, 13, 889-895.

[53] **Agard, N.J., Prescher, J.A., and Bertozzi, C.R.** (2005). A strain-promoted 3+2 azide-alkyne cycloaddition for covalent modification of biomolecules in living systems (vol 126, pg 15046, 2004), *Journal of the American Chemical Society*, 127, 11196-11196.

[54] **Haigh, J.D.** (1994). The role of stratospheric ozone in modulating the solar radiative forcing of climate, *Nature*, 370, 544-546.

[55] **Steinberg-Yfrach, G., Rigaud, J.L., Durantini, E.N., Moore, A.L., Gust, D., and Moore, T.A.** (1998). Light-driven production of atp catalysed by f0f1-atp synthase in an artificial photosynthetic membrane, *Nature*, 392, 479-482.

[56] **Brumer, P. and Shapiro, M.** (1986). Control of unimolecular reactions using coherent-light, *Chemical Physics Letters*, 126, 541-546.

[57] **Assion, A., Baumert, T., Bergt, M., Brixner, T., Kiefer, B., Seyfried, V., Strehle, M., and Gerber, G.** (1998). Control of chemical reactions by feedback-optimized phase-shaped femtosecond laser pulses, *Science*, 282, 919-922.

[58] **Wang, M.L., Han, K.L., and He, G.Z.** (1998). Product rotational polarization in photo-initiated bimolecular reactions a+bc: Dependence on the character of the potential energy surface for different mass combinations, *Journal of Physical Chemistry A*, 102, 10204-10210.

[59] **Crim, F.F.** (1996). Bond-selected chemistry: Vibrational state control of photodissociation and bimolecular reaction, *Journal of Physical Chemistry*, 100, 12725-12734.

[60] **David, P.G. and Dasilva, P.A.C.** (1985). Photoredox chemistry of chloro and bromo complexes of copper(ii) in methanolic medium, *Bulletin of the Chemical Society of Japan*, 58, 3566-3569.

[61] **Harmand, L., Cadet, S., Kauffmann, B., Scarpantonio, L., Batat, P., Jonusauskas, G., McClenaghan, N.D., Lastecoueres, D., and Vincent, J.-M.** (2012). Copper catalyst activation driven by photoinduced electron transfer: A prototype photolatent click catalyst, *Angewandte Chemie-International Edition*, 51, 7137-7141.

[62] **Agard, N.J., Prescher, J.A., and Bertozzi, C.R.** (2004). A strain-promoted 3+2 azide-alkyne cycloaddition for covalent modification of blomolecules in living systems, *Journal of the American Chemical Society*, 126, 15046-15047.

[63] **Baskin, J.M., Prescher, J.A., Laughlin, S.T., Agard, N.J., Chang, P.V., Miller, I.A., Lo, A., Codelli, J.A., and Bertozzi, C.R.** (2007). Copper-free click chemistry for dynamic in vivo imaging, *Proceedings of the National Academy of Sciences of the United States of America*, 104, 16793-16797.

[64] **Devaraj, N.K., Dinolfo, P.H., Chidsey, C.E.D., and Collman, J.P.** (2006). Selective functionalization of independently addressed microelectrodes by electrochemical activation and deactivation of a coupling catalyst, *Journal of the American Chemical Society*, 128, 1794-1795.

[65] **Ku, S.-Y., Wong, K.-T., and Bard, A.J.** (2008). Surface patterning with fluorescent molecules using click chemistry directed by scanning electrochemical microscopy, *Journal of the American Chemical Society*, 130, 2392-2393.

[66] **Panigrahi, S., Basu, S., Praharaj, S., Pande, S., Jana, S., Pal, A., Ghosh, S.K., and Pal, T.** (2007). Synthesis and size-selective catalysis by supported gold nanoparticles: Study on heterogeneous and homogeneous catalytic process, *Journal of Physical Chemistry C*, 111, 4596-4605.

[67] **Rance, G.A., Solomonsz, W.A., and Khlobystov, A.N.** (2013). Click chemistry in carbon nanoreactors, *Chemical Communications*, 49, 1067-1069.

[68] **Orgueira, H.A., Fokas, D., Isome, Y., Chan, P. C.-M. and Baldino, C. M.** ((2005)). *Tetrahedron Letters*, 46, 2911.

[69] **Pachón, L.D., Maarseveen, H. H. van and Rothenberg, G.** ((2005)). *Adv. Synth. Catal.*, 347, 811.

[70] **Gerard, B., Ryan, J., Beeler, A.B., and Porco, J.A., Jr.** (2006). Synthesis of 1,4,5-trisubstituted-1,2,3-triazoles by copper-catalyzed cycloaddition-coupling of azides and terminal alkynes, *Tetrahedron*, 62, 6405-6411.

[71] **Angell, Y. and Burgess, K.** (2007). Base dependence in copper-catalyzed huisgen reactions: Efficient formation of bistriazoles, *Angewandte Chemie-International Edition*, 46, 3649-3651.

[72] **Meldal, M.** (2008). Polymer "clicking" by cuaac reactions, *Macromolecular Rapid Communications*, 29, 1016-1051.

[73] **Appukkuttan, P., Dehaen, W., Fokin, V.V., and Van der Eycken, E.** (2004). A microwave-assisted click chemistry synthesis of 1,4-disubstituted 1,2,3-triazoles via a copper(i)-catalyzed three-component reaction, *Organic Letters*, 6, 4223-4225.

[74] **Cintas, P., Barge, A., Tagliapietra, S., Boffa, L., and Cravotto, G.** (2010). Alkyne-azide click reaction catalyzed by metallic copper under ultrasound, *Nature Protocols*, 5, 607-616.

[75] **Cravotto, G., Fokin, V.V., Garella, D., Binello, A., Boffa, L., and Barge, A.** (2010). Ultrasound-promoted copper-catalyzed azide-alkyne cycloaddition, *Journal of Combinatorial Chemistry*, 12, 13-15.

[76] **Nolte, C., Mayer, P., and Straub, B.F.** (2007). Isolation of a copper(i) triazolide: A"click" intermediate", *Angewandte Chemie-International Edition*, 46, 2101-2103.
[77] **Meldal, M. and Tornoe, C.W.** (2008). Cu-catalyzed azide-alkyne cycloaddition, *Chemical Reviews*, 108, 2952-3015.
[78] **Kolodziejczak-Radzimska, A. and Jesionowski, T.** (2014). Zinc oxide-from synthesis to application: A review, *Materials*, 7, 2833-2881.
[79] Vaseem, M., Umar, A., Hahn, Y. B., *Zno nanoparticles: Growth,properties, and applications*
[80] **Zheng, M., Davidson, F., and Huang, X.Y.** (2003). Ethylene glycol monolayer protected nanoparticles for eliminating nonspecific binding with biological molecules, *Journal of the American Chemical Society*, 125, 7790-7791.
[81] **Ferrari, M.** (2005). Cancer nanotechnology: Opportunities and challenges, *Nature Reviews Cancer*, 5, 161-171.
[82] **Reynolds, D.C., Look, D.C., Jogai, B., Hoelscher, J.E., Sherriff, R.E., Harris, M.T., and Callahan, M.J.** (2000). Time-resolved photoluminescence lifetime measurements of the gamma(5) and gamma(6) free excitons in zno, *Journal of Applied Physics*, 88, 2152-2153.
[83] **Lee, J.S., Park, K., Kang, M.I., Park, I.W., Kim, S.W., Cho, W.K., Han, H.S., and Kim, S.** (2003). Zno nanomaterials synthesized from thermal evaporation of ball-milled zno powders, *Journal of Crystal Growth*, 254, 423-431.
[84] **Baxter, J.B. and Aydil, E.S.** (2005). Nanowire-based dye-sensitized solar cells, *Applied Physics Letters*, 86.
[85] **Sawai, J., Kawada, E., Kanou, F., Igarashi, H., Hashimoto, A., Kokugan, T., and Shimizu, M.** (1996). Detection of active oxygen generated from ceramic powders having antibacterial activity, *Journal of Chemical Engineering of Japan*, 29, 627-633.
[86] **Segets, D., Gradl, J., Taylor, R.K., Vassilev, V., and Peukert, W.** (2009). Analysis of optical absorbance spectra for the determination of zno nanoparticle size distribution, solubility, and surface energy, *Acs Nano*, 3, 1703-1710.
[87] **Bacaksiz, E., Parlak, M., Tomakin, M., Ozcelik, A., Karakiz, M., and Altunbas, M.** (2008). The effects of zinc nitrate, zinc acetate and zinc chloride precursors on investigation of structural and optical properties of zno thin films, *Journal of Alloys and Compounds*, 466, 447-450.
[88] **Wang, J., Cao, J.M., Fang, B.Q., Lu, P., Deng, S.G., and Wang, H.Y.** (2005). Synthesis and characterization of multipod, flower-like, and shuttle-like zno frameworks in ionic liquids, *Materials Letters*, 59, 1405-1408.
[89] **Wang, Z.L.** (2008). Splendid one-dimensional nanostructures of zinc oxide: A new nanomaterial family for nanotechnology, *Acs Nano*, 2, 1987-1992.
[90] **Chaari, M. and Matoussi, A.** (2012). Electrical conduction and dielectric studies of zno pellets, *Physica B-Condensed Matter*, 407, 3441-3447.
[91] **Ozgur, U., Alivov, Y.I., Liu, C., Teke, A., Reshchikov, M.A., Dogan, S., Avrutin, V., Cho, S.J., and Morkoc, H.** (2005). A comprehensive review of zno materials and devices, *Journal of Applied Physics*, 98.
[92] **Ludi, B. and Niederberger, M.** (2013). Zinc oxide nanoparticles: Chemical mechanisms and classical and non-classical crystallization, *Dalton Transactions*, 42, 12554-12568.

[93] **Hahn, Y.-B.** (2011). Zinc oxide nanostructures and their applications, *Korean Journal of Chemical Engineering*, 28, 1797-1813.
[94] **Banerjee, D., Lao, J.Y., Wang, D.Z., Huang, J.Y., Ren, Z.F., Steeves, D., Kimball, B., and Sennett, M.** (2003). Large-quantity free-standing zno nanowires, *Applied Physics Letters*, 83, 2061-2063.
[95] **Frade, T., Melo Jorge, M.E., and Gomes, A.** (2012). One-dimensional zno nanostructured films: Effect of oxide nanoparticles, *Materials Letters*, 82, 13-15.
[96] **Wahab, R., Ansari, S.G., Kim, Y.-S., Seo, H.-K., and Shin, H.-S.** (2007). Room temperature synthesis of needle-shaped zno nanorods via sonochemical method, *Applied Surface Science*, 253, 7622-7626.
[97] **Kong, X.Y., Ding, Y., Yang, R., and Wang, Z.L.** (2004). Single-crystal nanorings formed by epitaxial self-coiling of polar nanobelts, *Science*, 303, 1348-1351.
[98] **Pan, Z.W., Dai, Z.R., and Wang, Z.L.** (2001). Nanobelts of semiconducting oxides, *Science*, 291, 1947-1949.
[99] **Wu, J.J., Liu, S.C., Wu, C.T., Chen, K.H., and Chen, L.C.** (2002). Heterostructures of zno-zn coaxial nanocables and zno nanotubes, *Applied Physics Letters*, 81, 1312-1314.
[100] **Liu, J.P., Huang, X.T., Duan, J.X., Ai, H.H., and Tu, P.H.** (2005). A low-temperature synthesis of multiwhisker-based zinc oxide micron crystals, *Materials Letters*, 59, 3710-3714.
[101] **Huang, Y.H., He, J., Zhang, Y., Dai, Y., Gu, Y.S., Wang, S., and Zhou, C.** (2006). Morphology, structures and properties of zno nanobelts fabricated by zn-powder evaporation without catalyst at lower temperature, *Journal of Materials Science*, 41, 3057-3062.
[102] **Cui, J.** (2012). Zinc oxide nanowires, *Materials Characterization*, 64, 43-52.
[103] **Xu, T., Ji, P., He, M., and Li, J.** (2012). Growth and structure of pure zno micro/nanocombs, *Journal of Nanomaterials*.
[104] **Chiu, W.S., Khiew, P.S., Cloke, M., Isa, D., Tan, T.K., Radiman, S., Abd-Shukor, R., Abd Hamid, M.A., Huang, N.M., Lim, H.N., and Chia, C.H.** (2010). Photocatalytic study of two-dimensional zno nanopellets in the decomposition of methylene blue, *Chemical Engineering Journal*, 158, 345-352.
[105] **Jose-Yacaman, M., Gutierrez-Wing, C., Miki, M., Yang, D.Q., Piyakis, K.N., and Sacher, E.** (2005). Surface diffusion and coalescence of mobile metal nanoparticles, *Journal of Physical Chemistry B*, 109, 9703-9711.
[106] **Polshettiwar, V., Baruwati, B., and Varma, R.S.** (2009). Self-assembly of metal oxides into three-dimensional nanostructures: Synthesis and application in catalysis, *Acs Nano*, 3, 728-736.
[107] Jagadish, C. and Pearton, S.J. *Zinc oxide bulk, thin films and nanostructures processing, properties and applications*. 2006 [cited; Available from: http://www.engineeringvillage.com/controller/servlet/OpenURL?genre=book&isbn=9780080447223.
[108] **Lee, G.H., Yamamoto, Y., Kourogi, M., and Ohtsu, M.** (2001). Blue shift in room temperature photoluminescence from photo-chemical vapor deposited zno films, *Thin Solid Films*, 386, 117-120.
[109] **Reeber, R.R.** (1970). Lattice parameters of zno from 4.2 degrees to 296 degrees k, *Journal of Applied Physics*, 41, 5063-&.

[110] **Hahn, Y.-B. and Umar, A.**, *Metal oxide nanostructures and their applications*. 2010, Stevenson Ranch, Calif.: American Scientific Publishers.
[111] **Kuoni, A., Holzherr, R., Boillat, M., and de Rooij, N.F.** (2003). Polyimide membrane with zno piezoelectric thin film pressure transducers as a differential pressure liquid flow sensor, *Journal of Micromechanics and Microengineering*, 13, S103-S107.
[112] **Blom, F.R., Yntema, D.J., Vandepol, F.C.M., Elwenspoek, M., Fluitman, J.H.J., and Popma, T.J.A.** (1990). Thin-film zno as micromechanical actuator at low-frequencies, *Sensors and Actuators a-Physical*, 21, 226-228.
[113] **Song, R.-Q., Xu, A.-W., Deng, B., Li, Q., and Chen, G.-Y.** (2007). From layered basic zinc acetate nanobelts to hierarchical zinc oxide nanostructures and porous zinc oxide nanobelts, *Advanced Functional Materials*, 17, 296-306.
[114] **Polarz, S., Orlov, A.V., Schueth, F., and Lu, A.-H.** (2007). Preparation of high-surface-area zinc oxide with ordered porosity, different pore sizes, and nanocrystalline walls, *Chemistry-a European Journal*, 13, 592-597.
[115] **Khan, S.B., Faisal, M., Rahman, M.M., and Jamal, A.** (2011). Low-temperature growth of zno nanoparticles: Photocatalyst and acetone sensor, *Talanta*, 85, 943-949.
[116] **Alvarez, S.G. and Alvarez, M.T.** (1997). A practical procedure for the synthesis of alkyl azides at ambient temperature in dimethyl sulfoxide in high purity and yield, *Synthesis-Stuttgart*, 413-414.
[117] **Meudtner, R.M., Ostermeier, M., Goddard, R., Limberg, C., and Hecht, S.** (2007). Multifunctional "clickates" as versatile extended heteroaromatic building blocks: Efficient synthesis via click chemistry, conformational preferences, and metal coordination, *Chemistry - A European Journal*, 13, 9834-9840.

^{1}H NMR AND ^{13}C NMR SPECTRA

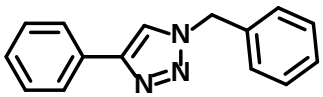

4-Benzyl-1-phenyl-1*H*-1,2,3-triazole (3a). White solid. Yield 98%. ^{1}H NMR (500 MHz, $CDCl_3$): δ 7.80 (d, 2H), 7.67 (s, 1H), 7.42-7.27 (m, 8H), 5.59 (s, 2H); ^{13}C NMR (125 MHz, $CDCl_3$): δ 148.2, 134.7, 130.6, 129.1, 128.8, 128.7, 128.2, 128.1, 125.7, 119.4, 54.2.

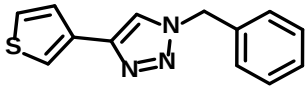

1-Benzyl-4-(thiophen-3-yl)-1*H*-1,2,3-triazole (3b). White solid. Yield 90%. ^{1}H NMR (500 MHz, $CDCl_3$): δ 7.65 (m, 1H), 7.56 (s, 1H), 7.43-7.35 (m, 5H), 7.30 (m, 2H), 5.57 (s, 2H); ^{13}C NMR (125 MHz, $CDCl_3$): δ 144.4, 134.6, 131.8, 129.1, 128.8, 128.0, 126.3, 125.8, 121.1, 119.3, 54.2.

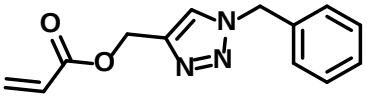

(1-Benzyl-1*H*-1,2,3-triazol-4-yl)methyl acrylate (3c). Pale yellow oil. Yield 98%. ^{1}H NMR (500 MHz, $CDCl_3$): δ 7.54 (s, 1H), 7.39-7.27 (m, 5H), 6.44-6.40 (m, 1H), 6.14-6.09 (m, 1H), 5.97-5.94 (m, 1H), 5.53 (s, 2H), 5.28 (s, 2H); ^{13}C NMR (125 MHz, $CDCl_3$): δ 166.1, 143.2, 134.24, 131.4, 129.1, 128.8, 128.1, 127.9, 126.6, 57.7, 54.2.

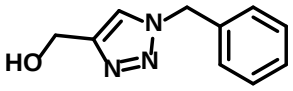

(1-Benzyl-1*H*-1,2,3-triazol-4-yl)methanol (3d). White solid. Yield 81%. ^{1}H NMR (500 MHz, $CDCl_3$): δ 7.72 (s, 1H), 7.47-7.44 (d, 2H), 7.42-7.27 (m, 3H), 5.60 (s, 2H), 5.30 (s, 1H), 4.78 (s, 2H); ^{13}C NMR (125 MHz, $CDCl_3$): δ 140.1, 134.7, 129.4, 128.4, 128.1, 121.4, 56.7, 51.7.

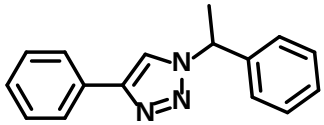

4-Phenyl-1-(1-phenylethyl)-1*H*-1,2,3-triazole (3e). White solid. Yield 92%. ^{1}H NMR (500 MHz, $CDCl_3$): δ 8.18 (d, 1H), 7.95 (s, 1H), 7.85 (d, 2H), 7.65-7.34 (m, 6H), 7.15 (d, 1H), 6.01 (s, 2H); ^{13}C NMR (125 MHz, $CDCl_3$): δ 147.7, 139.9, 130.7, 129.0, 128.7, 128.5, 128.0, 126.5, 125.6, 118.3, 60.3.

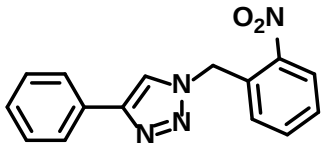

1-(2-Nitrobenzyl)-4-phenyl-1*H*-1,2,3-triazole (3f). White solid. Yield 98%. ^{1}H NMR (500 MHz, $CDCl_3$): δ 8.18 (d, 1H), 7.95 (s, 1H), 7.85 (d, 2H), 7.65-7.34 (m,

6H), 7.15 (d, 1H), 6.01 (s, 2H); ^{13}C NMR (125 MHz, $CDCl_3$): δ 148.4, 134.4, 133.9, 132.5, 130.7, 129.6, 129.2, 128.8, 128.7, 128.3, 126.3, 125.8, 135.3, 120.5, 50.9.

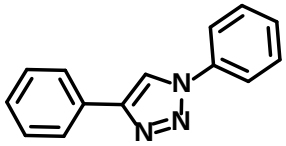

1,4-Diphenyl-1*H*-1,2,3-triazole (3g). Pale yellow oil. Yield 99%. ^{1}H NMR (500 MHz, $CDCl_3$): δ 8.21 (s, 1H), 7.94 (d, 2H), 7.81 (d, 2H), 7.58-7.34 (m, 6H); ^{13}C NMR (125 MHz, $CDCl_3$): δ 148.4, 137.0, 132.5, 130.3, 129.8, 128.9, 128.4, 125.9, 120.54, 117.56.

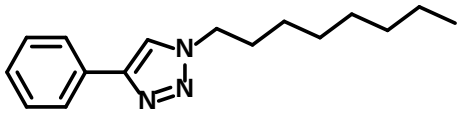

1-Octyl-4-phenyl-1*H*-1,2,3-triazole (3h). White solid. Yield 64%. ^{1}H NMR (500 MHz, $CDCl_3$): δ 7.85 (d, 2H), 7.75 (s, 1H), 7.45-7.32 (m, 3H), 4.40 (t, 2H), 1.96 (m, 2H), 1.36-1.27 (m, 10H), 0.89 (t, 3H); ^{13}C NMR (125 MHz, $CDCl_3$): δ 147.8, 137.7, 128.8, 128.0, 127.7, 119.3, 50.4, 31.7, 30.3, 28.9, 26.5, 22.6, 14.0.

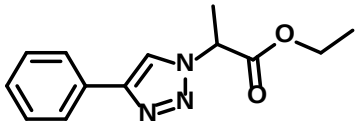

Ethyl 2-(4-phenyl-1*H*-1,2,3-triazol-1-yl)propanoate (3i). White solid. Yield 84%. ^{1}H NMR (500 MHz, $CDCl_3$): δ 8.00 (s, 1H), 7.86 (d, 2H), 7.44-7.41 (t, 2H), 7.40-7.28 (t, 1H), 5.56 (d, 1H), 4.25-4.20 (m, 2H), 1.88 (d, 3H), 1.29-1.26 (t, 3H); ^{13}C NMR (125 MHz, $CDCl_3$): δ 169.4, 147.7, 130.5, 128.8, 128.2, 125.8, 118.9, 116.4, 62.4, 58.4, 18.4, 13.9.

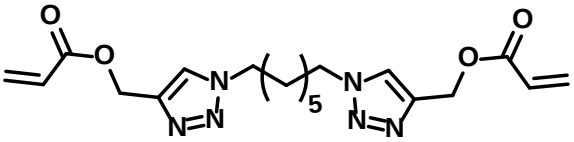

(Heptane-1,7-diylbis(1*H*-1,2,3-triazole-1,4-diyl))bis(methylene) diacrylate (3k). White solid. Yield 80%. ^{1}H NMR (500 MHz, $CDCl_3$): δ 7.60 (s, 2H), 6.45 (d, 2H), 6.16 (m, 2H), 5.86 (d, 2H), 5.30 (s, 4H), 4.33 (t, 4H), 1.89 (t, 4H), 1.32 (m, 6H); ^{13}C NMR (125 MHz, $CDCl_3$): δ 166.0, 142.5, 131.4, 128.0, 123.8, 123.7, 123.3, 57.7, 50.0, 49.9, 30.1, 28.2, 26.0.

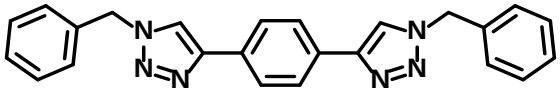

1,4-Bis(1-benzyl-1*H*-1,2,3-triazol-4-yl)benzene (3l). White solid. Yield 50%. ^{1}H NMR (500 MHz, $CDCl_3$): δ 7.77 (d, 4H), 7.68 (s, 2H), 7.52 (d, 4H), 7.42-7.33 (m, 10H), 5.58 (s, 4H); ^{13}C NMR (125 MHz, $CDCl_3$): δ 147.5, 134.5, 132.6, 130.9, 129.2, 128.8, 128.1, 125.5, 121.7, 119.8, 54.3.

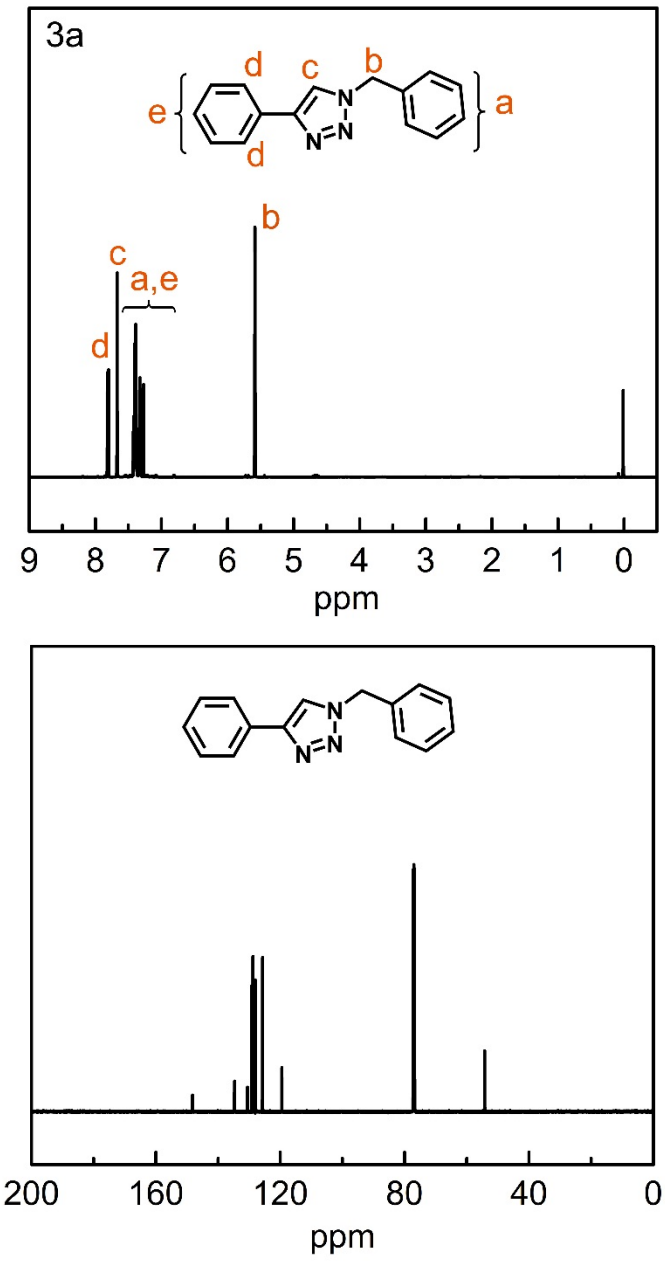
3a
d
c
b
e
a
d
N
N
N
b
c
a,e
d
9
8
7
6
5
4
3
2
1
0
ppm
N
N
N
200
160
120
80
40
0
ppm

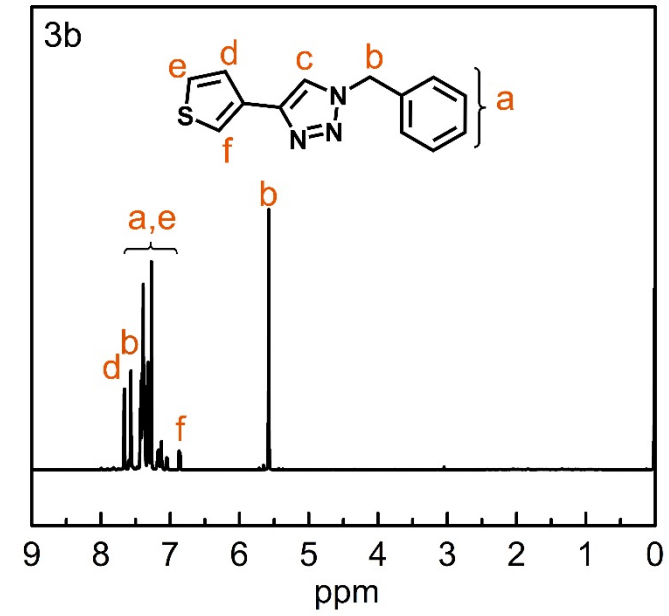
3b
e
d
c
b
a
f
S
N
N=N
b
a,e
d
b
f
9
8
7
6
5
4
3
2
1
0
ppm

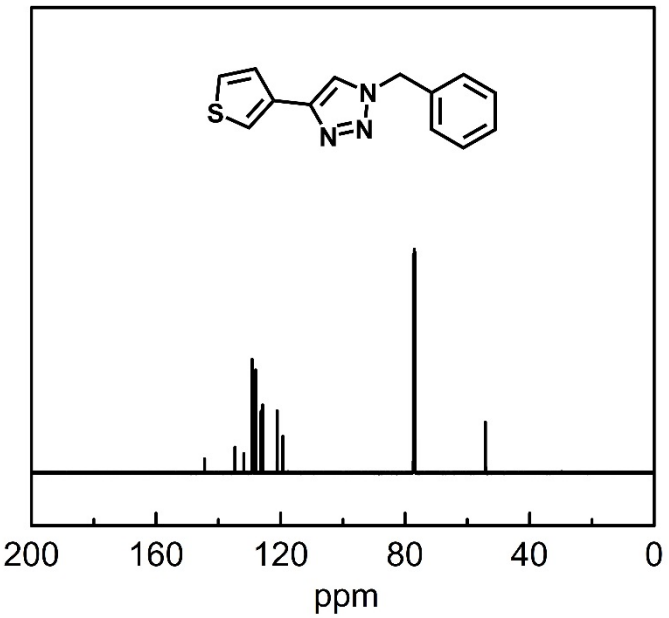
S
N
N=N
200
160
120
80
40
0
ppm

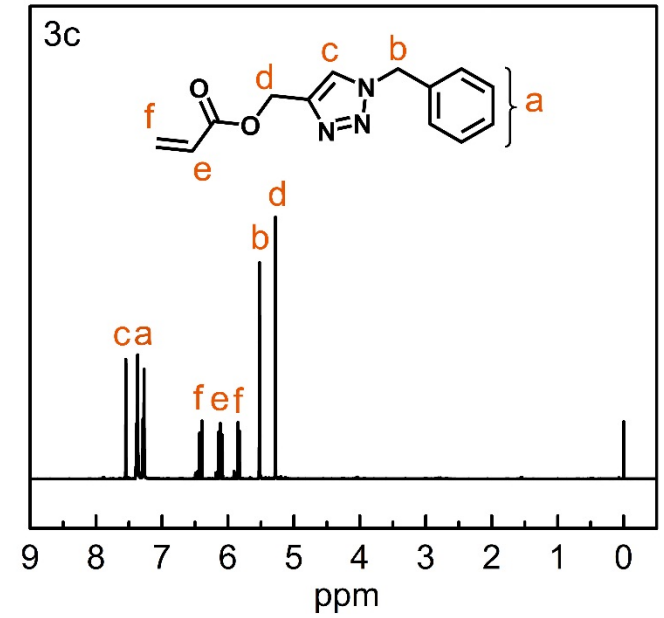
3c
c
b
d
a
f
e
d
b
c a
f e f
9 8 7 6 5 4 3 2 1 0
ppm

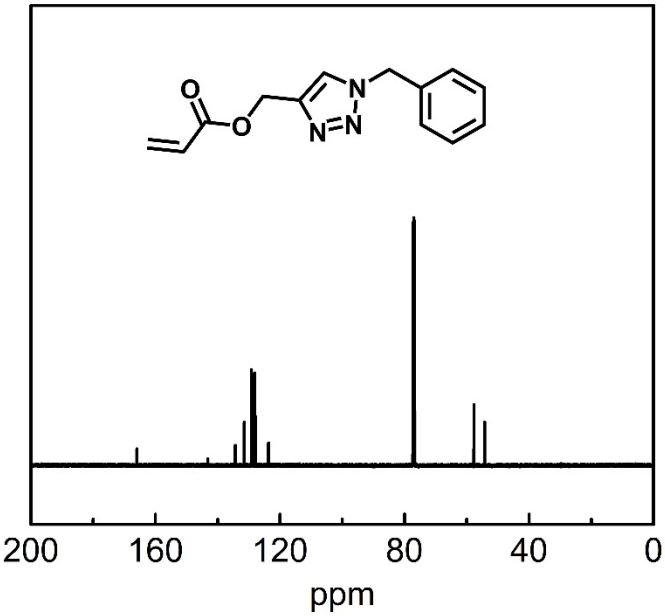
200 160 120 80 40 0
ppm

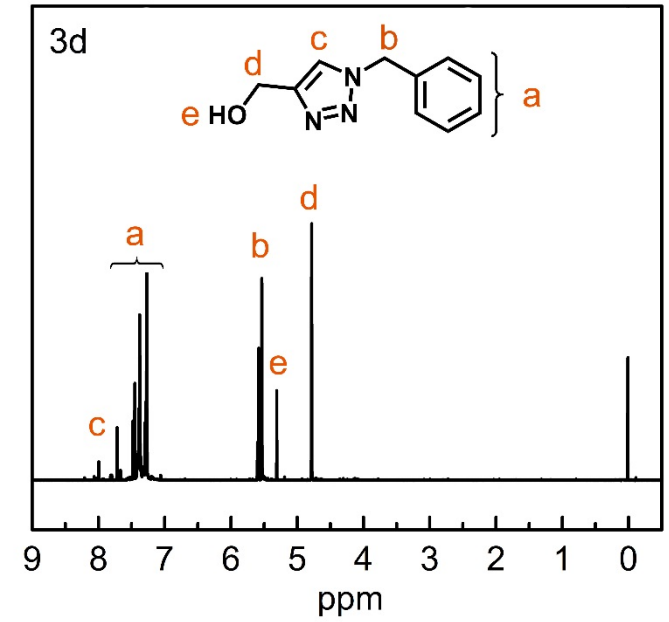
3d
c
b
d
e HO
N
N=N
a
d
a
b
e
c
9
8
7
6
5
4
3
2
1
0
ppm

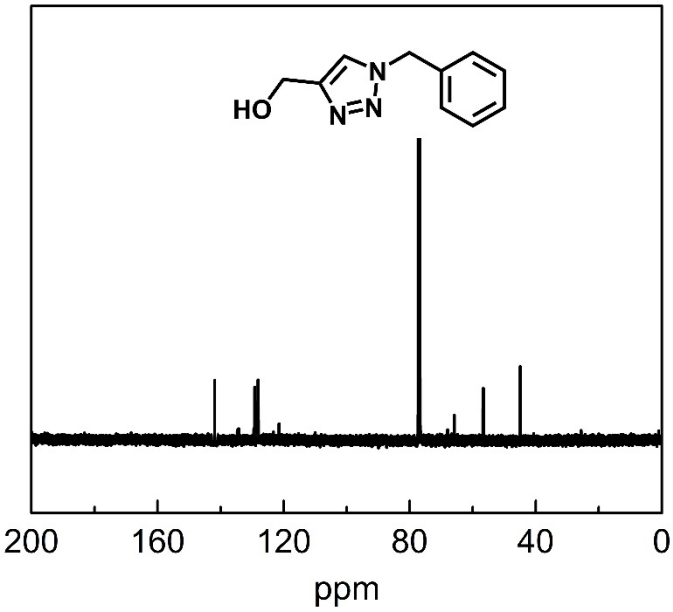
HO
N
N=N
200
160
120
80
40
0
ppm

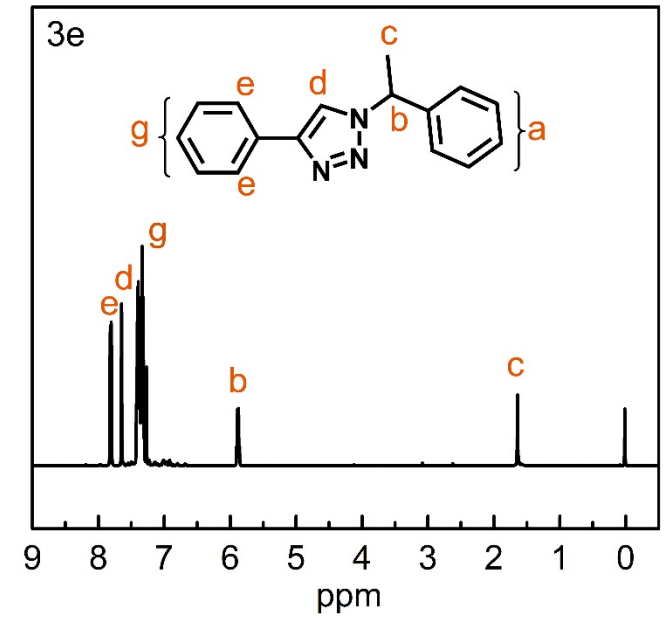
3e
c
e
d
g
b
a
e
N
N
N
g
d
e
b
c
9
8
7
6
5
4
3
2
1
0
ppm

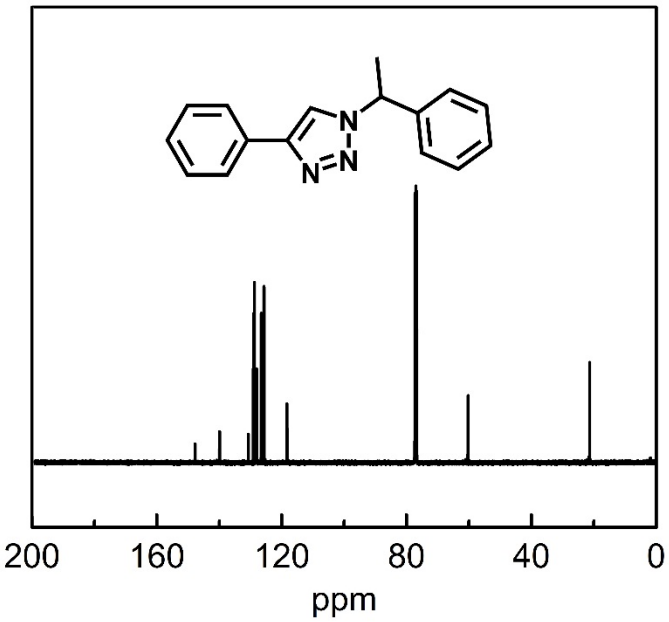
N
N
N
200
160
120
80
40
0
ppm

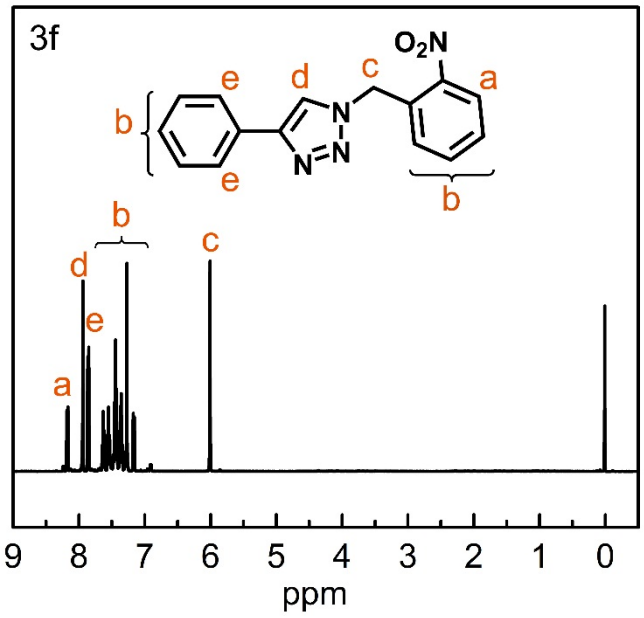
3f
O_2N
a
b
c
d
e
9 8 7 6 5 4 3 2 1 0
ppm

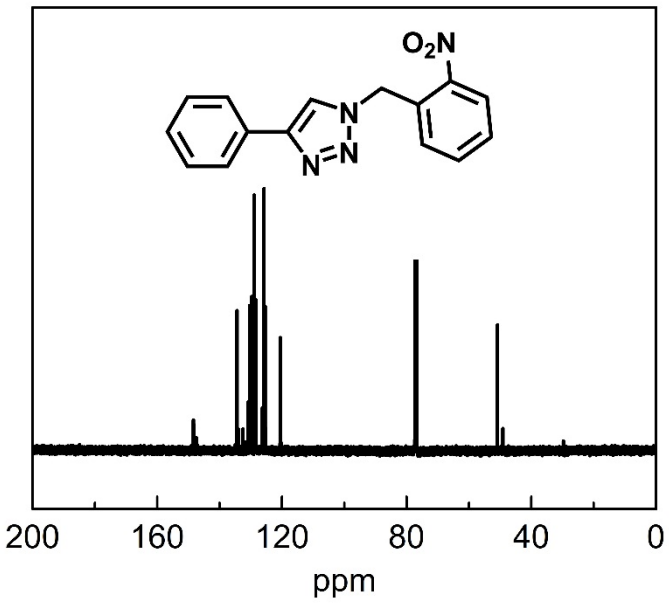
O_2N
200 160 120 80 40 0
ppm

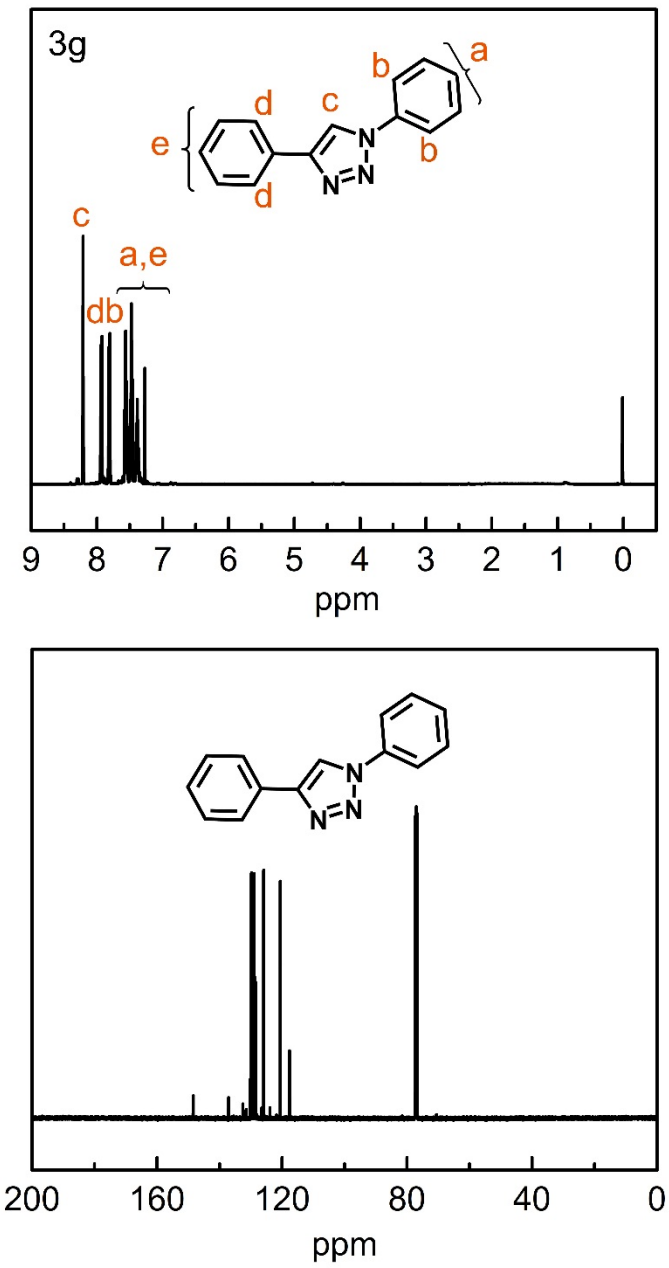
3g
a
b
c
d
e
b
d
d
c
a,e
db
9
8
7
6
5
4
3
2
1
0
ppm
200
160
120
80
40
0
ppm

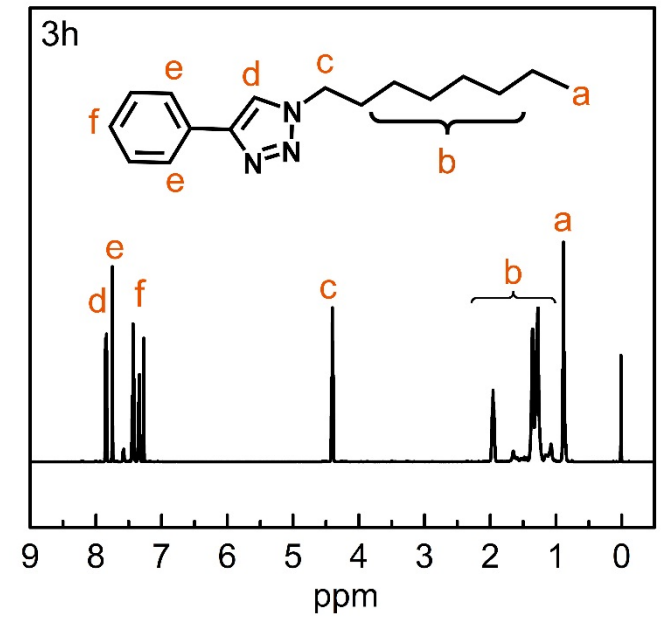
3h
e
d
c
a
f
e
b
a
e
b
d
f
c
9
8
7
6
5
4
3
2
1
0
ppm

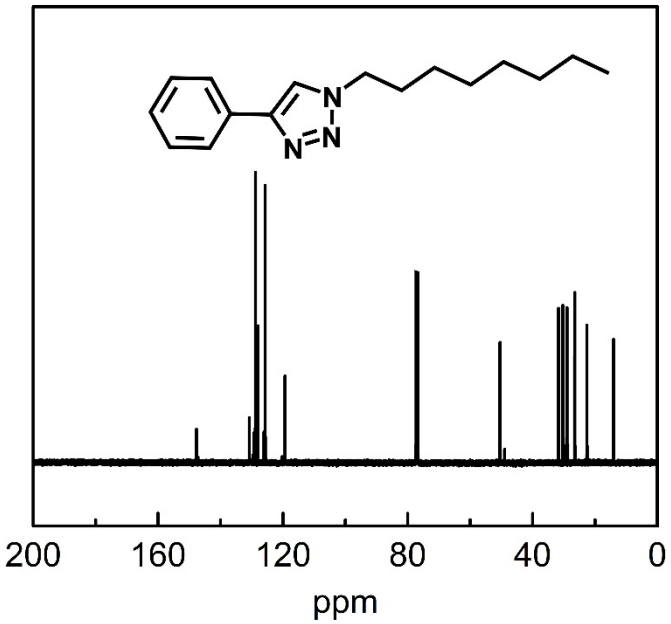
200
160
120
80
40
0
ppm

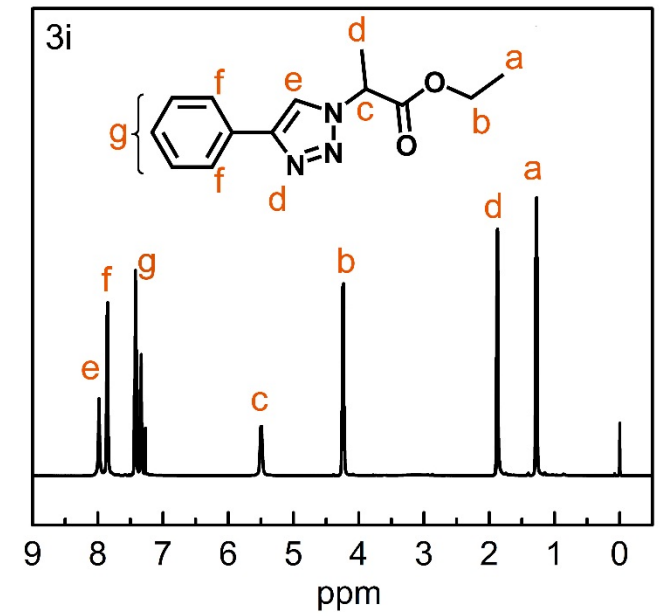
3i
d
a
f
e
c
b
g
f
d
d
a
f
g
b
e
c
9
8
7
6
5
4
3
2
1
0
ppm

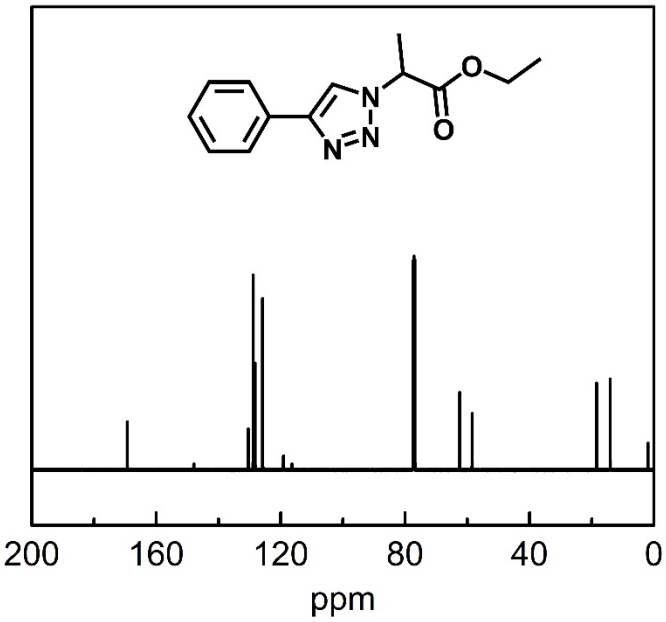
200
160
120
80
40
0
ppm

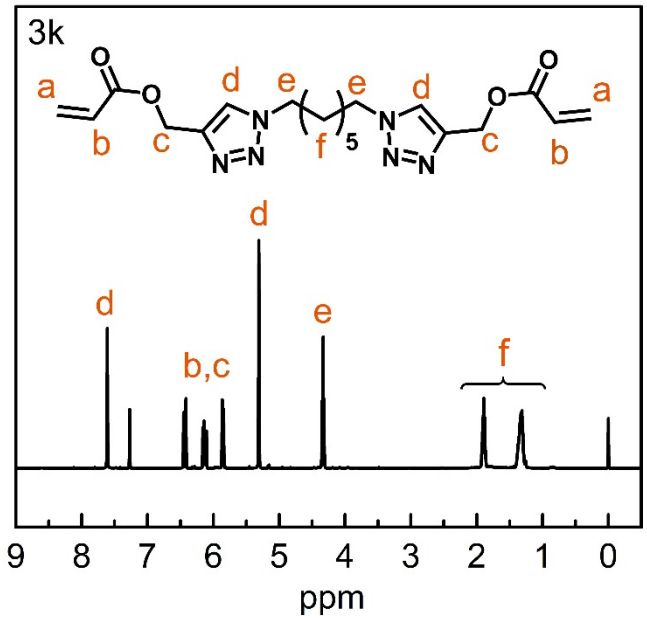
3k
a
b
c
d
e
f
5
d
d
e
b,c
f
9 8 7 6 5 4 3 2 1 0
ppm

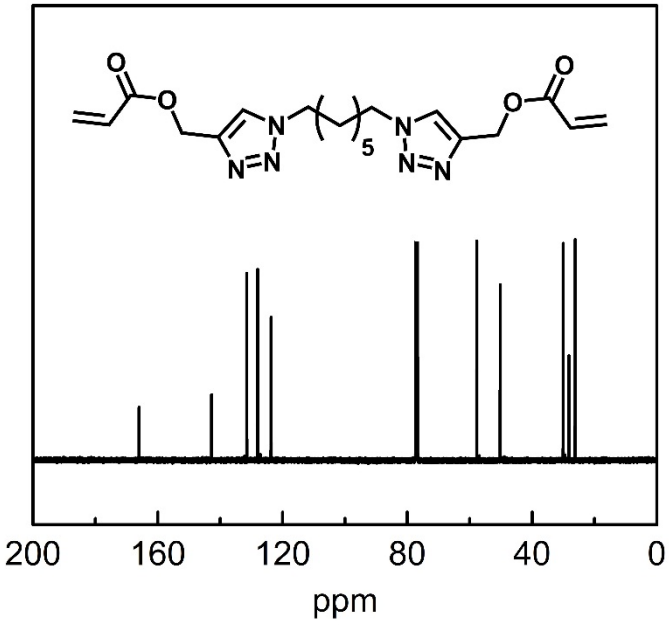
5
200 160 120 80 40 0
ppm

CURRICULUM VITAE

Name Surname: Özde YETİŞKİN

Place and Date of Birth: Sarıyer / 18.11.1987

E-Mail: ozde.yetiskin87@gmail.com

EDUCATION:

B.Sc.: Marmara University, Secondary Education, Science, Maths Department of Chemistry Teacher Education, 2008-2013

M.Sc.: Istanbul Technical University, Faculty of Science and Letters, Department of Chemistry (2013-…)

PUBLICATIONS AND PRESENTATIONS ON THE THESIS:

- **Yetiskin O.**, Dadashi-Silab S., Khan S. B., Asiri A. B. and Yagcı Y. Visible light-induced copper(I) catalyzed azide-alkine cycloaddition with zinc oxide semiconductor nanoparticles. *Asian Journal of Organic Chemistry, 2015, 4(5), 442-444.*
- **Yetiskin O**., Dadashi-Silab S., Khan S. B., Asiri A. B. and Yagcı Y. Visible light-induced copper(I)-catalyzed azide-alkyne cycloaddition with zinc oxide semiconductor nanoparticles. *POLYCHEM 2015 - International Symposium on Polymers from Renewable Resouces, May 8, 2015, Boğaziçi Universitiy,* Istanbul, TURKEY. *(Poster presentation)*
- **Yetiskin O**., Dadashi-Silab S. , Khan S. B., Asiri A. B. and Yagcı Y. ZnO yarı-iletken nanopartikülleri kullanılarak heterojen fotokataliz sistemi ile azid-alkin "çıt-çıt" reaksiyonu. *27. National Chemistry Congress, 23-28 August, 2015,* Çanakkale, TURKEY. *(Poster presentation)*
- **Yetiskin O**., Dadashi-Silab S., Khan S. B., Asiri A. B. and Yagcı Y. Photoinduced copper-catalyzed click chemistry by semiconductor nanoparticles: A macromolecular approach. *BPS'15 - Bayreuth Polymer Symposium, 20-22 October, 2015,* Bayreuth, GERMANY. *(Poster presentation)*